iScience

CellPress
OPEN ACCESS

Review

Mechanical sensors based on two-dimensional materials: Sensing mechanisms, structural designs and wearable applications

Tingting Yang,[1] Xin Jiang,[2] Yuehua Huang,[3] Qiong Tian,[4] Li Zhang,[5] Zhaohe Dai,[6] and Hongwei Zhu[2,*]

SUMMARY

Compared with bulk materials, atomically thin two-dimensional (2D) crystals possess a range of unique mechanical properties, including relatively high in-plane stiffness and large bending flexibility. The atomic 2D building blocks can be reassembled into precisely designed heterogeneous composite structures of various geometries with customized mechanical sensing behaviors. Due to their small specific density, high flexibility, and environmental adaptability, mechanical sensors based on 2D materials can conform to soft and curved surfaces, thus providing suitable solutions for functional applications in future wearable devices. In this review, we summarize the latest developments in mechanical sensors based on 2D materials from the perspective of function-oriented applications. First, typical mechanical sensing mechanisms are introduced. Second, we attempt to establish a correspondence between typical structure designs and the performance/multi-functions of the devices. Afterward, several particularly promising areas for potential applications are discussed, following which we present perspectives on current challenges and future opportunities

INTRODUCTION

Two-dimensional (2D) materials such as semi-metallic graphene, insulating hexagonal boron nitride (hBN), semiconducting molybdenum disulfide (MoS_2), and many more, are a new class of atomically thin materials with a range of unusual mechanical and electronic properties (Novoselov et al., 2016; Zhang et al., 2018a, 2018b In general, 2D materials are mechanically robust yet extremely compliant. For instance, although graphene has shown exceptional in-plane Young's modulus, its bending rigidity is just comparable to that of a lipid layer (Wei et al., 2013), breaking down classical plate theories. Recent studies further demonstrate that the bending stiffness of multilayer 2D crystals is also much more compliant than the classical plate prediction as the van der Waals (vdW) interactions between adjacent 2D layers allow interlayer shear and slippage (Falin et al., 2017; Han et al., 2020; Kumar et al., 2016; Wang et al., 2019a; Wei et al., 2016). Another intriguing mechanical advantage of 2D crystals arises from the capability of sustaining much larger mechanical strains before failure (Akinwande et al., 2017; Androulidakis et al., 2018; Lee et al., 2008), compared with traditional bulk crystals, including their bulk counterparts. In addition to the mechanical compliance, most 2D materials also possess good electrical properties, such as tunable band gap and high mobility (Cheng et al., 2019). Meanwhile, 2D materials are compatible with large-area processing technologies, leading to highly functional and low-cost next-generation wearable electronic devices (Chen et al., 2017c; Hou et al., 2014; Jian et al., 2017; Park et al., 2016).

The mechanoelectrical coupling properties of 2D materials are closely related to their geometric dimensions. The sensing mechanism in these 2D sensing devices comes from different origins. At the microscopic scale, the stress or strain applied onto a crystalline 2D layer would alter its atomic lattice and electron band structure. Thereby, the electrical and photonic properties of the atomic layer (Chang et al., 2013; Hosseini et al., 2015a; Lloyd et al., 2016) can be directly adjusted, leading to mechanical deformation-sensitive properties. However, this principle becomes more complicated when the manufacturing process turns from microscopic into macroscopic scales as many mechanical and chemical subtleties appear. At the macroscopic scale, apart from the crystallography-dependent behavior (Huang et al., 2011), macroscopic structures (Chen et al., 2011; Yang et al., 2015), chemical functionalization (Eswaraiah et al., 2011; Zha et al., 2016), interlayer sliding interfaces (Li et al., 2016b; Liu et al., 2016a), substrate interaction (Yang et al., 2017b), size of 2D layer (Chen et al., 2016b), and

[1]Tribology Research Institute, School of Mechanical Engineering, Southwest Jiaotong University, Chengdu 610031, China

[2]State Key Lab of New Ceramics and Fine Processing, School of Materials Science and Engineering, Tsinghua University, Beijing 100084, China

[3]College of Engineering and Technology, Southwest University, Chongqing 400715, China

[4]Key Lab of Human-Machine Intelligence-Synergy Systems, Shenzhen Institutes of Advanced Technology Chinese Academy of Sciences, Shenzhen 518055, China

[5]Key Lab of Photochemical Conversion and Optoelectronic Materials, Technical Institute of Physics and Chemistry, Chinese Academy of Sciences, Beijing 100190, China

[6]Department of Aerospace Engineering and Engineering Mechanics, The University of Texas at Austin, Austin, TX 78712, USA

*Correspondence: hongweizhu@tsinghua.edu.cn

https://doi.org/10.1016/j.isci.2021.103728

substrate morphology (Zhu et al., 2014) can also modify its mechanoelectrical coupling properties. Besides, some 2D crystals present a piezoelectric effect with the ability to generate electric charges and potentials in response to the mechanical load (Dai et al., 2019a; Duerloo et al., 2012), and mechanical sensors based on the capacitive (Davidovikj et al., 2017; Kang et al., 2017) and triboelectric type (Chu et al., 2016) of 2D materials have also been widely reported. In the past years, the booming developments of sensing mechanisms, novel structure designs, and fabrication methods lead to continuous advance of 2D materials based mechanical sensors. The basic sensor performance parameters such as sensitivity and stretchability have been improved to a level that even exceeds those of the biological skin.

The realization of deterministic functions with high performance is the goal of constructing and assembling structural materials. Mechanical sensors based on 2D materials can be used in many aspects of daily life, and its development and popularization will greatly improve people's quality of life. For example, the inherent light weight of 2D crystals makes membranes made from these materials exhibit small inertia in nanoelectromechanical sensors, which allows them to react very quickly to mechanical stimuli and exhibit short response time and high sensitivity. Some useful information of 2D crystals based nanoelectromechanical sensors are referred to in several recent papers (Chen, 2013; Fan et al., 2019). Herein, we will only highlight the most representative characteristics of 2D materials in wearable mechanical sensing applications. For example, 2D materials based skin type (Yang et al., 2015; Zhang and Tao, 2019) and textile type (Cheng et al., 2015; Huang et al., 2019b) mechanical sensors are "worn" on the human body to realize long-term dynamic monitoring of human physiological information and provide comprehensive clinical diagnostic data or health information. Such wearable capability is also very useful for sensors to be installed at the end of the robot finger to convert the force stimulus information obtained by perception into digital information (Sun et al., 2019), which provides essential sensing feedback for robots to handle objects and use tools. In addition, some stirring properties (e.g., biocompatibility (Huang et al., 2019a), biodegradability (Zhang and Tao, 2019), superhydrophobic (Dinh et al., 2019), self-healing (D'Elia et al., 2015; Lin et al., 2019), self-powering (Wang et al., 2018), visualization (Deng et al., 2017; Yang et al., 2017b), gas permeability (Sun et al., 2018), flame retardancy (Wang et al., 2020a), acid alkali-resistance (Wang et al., 2020a)) have also been achieved, which further broaden the application scope of 2D materials based-wearable mechanical sensors. In the future, combining wearable sensors with machine learning and artificial intelligence technologies to build machine learning-assisted smart sensors will become the theme (Yao et al., 2020; Zhou et al., 2020), which further promote the growth of many emerging diversified application markets and boost the prosperity of the Internet of Things to a new level. The structural designs and wearable applications of mechanical sensors based on 2D materials are illustrated in Figure 1.

SENSING MECHANISMS AND PROPERTIES

Here, we mainly introduce piezoresistive, capacitive, piezoelectric, and triboelectric principles. A summary of 2D materials-based strain and pressure sensors is presented in Table 1.

Piezoresistive principle and sensing properties

The piezoresistive effect describes the ability of a material to generate resistance changes in response to the mechanical stimuli. Sensors based on the piezoresistive effect usually have the advantages of ease of manufacture and low cost and are widely used to realize cost-effective wearable electronic products. This section discusses the piezoresistive properties of 2D materials from the perspective of structure design. Based on the understanding from the literature and ourselves, we categorize these 2D structure types as laterally designed 2D crystal structures (Figure 2A), vertically designed 2D crystal structures (Figure 2B), and heterogeneously designed 2D crystal composite structures (Figure 2C). Such classification based on structural characteristics facilitates a detailed discussion of the physical and chemical interactions of the interfaces (essentially shear and adhesion) involved in the 2D system, which in turn regulates the piezoresistive performance of the sensor.

Laterally designed 2D crystal structures

Laterally designed 2D crystal structures include 2D single crystals, polycrystals, and in-plane heterostructures. The resulting structures feature strong bonding in the crystal plane, and applied mechanical loadings activate the in-plane straining or shearing of the crystal layer, thus modulating their in-plane electrical transport. 2D crystals, showing distinct piezoresistive properties, such as graphene (Bae et al., 2013), MoS_2 (Manzeli et al., 2015; Tsai et al., 2015), WSe_2 (Hosseini et al., 2015b), $MoSe_2$ (Hosseini et al., 2015b) or $PtSe_2$ (Wagner et al., 2018), would be promising for strain or pressure sensor applications. To take

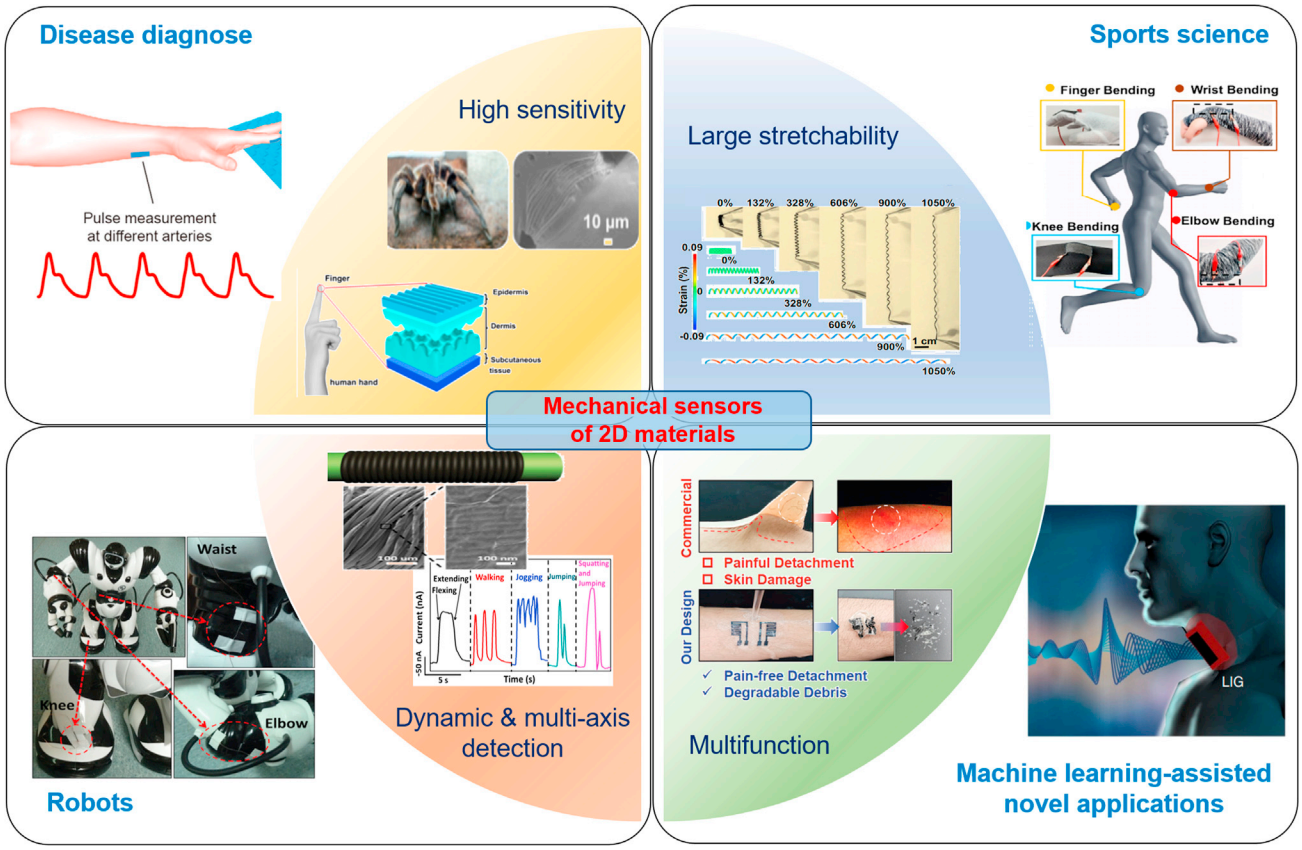

Figure 1. Structural designs and wearable applications of mechanical sensors based on 2D materials
Adapted from Refs. [(Cheng et al., 2015) (Dinh et al., 2019) (Wang et al., 2019b) (Zhang et al., 2020) (Zhang and Tao, 2019) (Yang et al., 2018) (Yao et al., 2020), (Tao et al., 2017)].

advantage of their inherent piezoresistive effects, high-quality CVD growth of 2D crystals is a prerequisite. However, imperfections or defects are usually introduced into 2D crystals during their synthesis (Banhart et al., 2010; Zhou et al., 2013). The atomic intercalations do not follow the perfect crystalline pattern and, thus, significantly alter the resultant lattice and structural response of 2D crystals to the mechanical load, resulting in physical and chemical properties of defective 2D crystals dissimilar to their pristine counterparts (Addou et al., 2015; Lee et al., 2015; Terrones et al., 2012).

On the other hand, one-dimensional (1D) line defects (grain boundaries) are usually inevitably introduced during the growth, especially when the lateral size of the material is much larger than the crystal grains (Van Der Zande et al., 2013; Yu et al., 2011). These grain boundaries help the 2D crystals to assemble into in-plane stitched architectures. The effect of the convergence region or grain boundaries on their mechanical and electrical properties tends to dominate over the crystal flake itself (Tsen et al., 2012; Zhang et al., 2013). Since the precise control of boundaries is challenging, the reported piezoresistive properties appeared scattered even for the same type of 2D material. For example, polycrystalline CVD graphene-based strain sensors have been obtained with a range of gauge factors from a few to several hundreds (Fu et al., 2011; Li et al., 2012a; Zhao et al., 2012), which seems to disaccord with the theoretical calculation results where the perfect graphene shows a gauge factor (GF) of less than 10 (Cocco et al., 2010; Gui et al., 2008; Ni et al., 2008). These reports suggest that it is difficult to guarantee the consistency of sensor performance based on the laterally designed 2D crystal structures.

Vertically designed 2D crystal structures

The bottom-up stacking of 2D crystals on top of each other presents a plethora of opportunities for mechanical sensing applications. The resulted structure features strong bonding in the crystal plane and weak bonding via vdW interactions between layers (Geim and Grigorieva, 2013; Liu et al., 2016c; Novoselov

Table 1. Strain and pressure sensors based on 2D materials

Transduction principles	Advantages/ Disadvantages	Sensed mechanical type	Key materials	Sensitivity (GF)	Range	Linearity	Vibration response	Cyclic stability	Application	Ref.
Piezoresistivity	√ High sensitivity √ Large measuring range √ Simple structures and fabrication techniques √ Low cost × Poor stability × Hysteresis effect × Temperature dependent	Strain	Functionalized graphene multilayers	200	0-2.5%	Linear	0-4 kHz	1000 cycles (0-1%)	Acoustic signal detection	(Yang et al., 2020)
			MXene/silver nanowire "brick" and poly (dopamine)/ Ni^{2+}"mortar"	256.1 (0-15%) 433.3 (15-35%) 1160.8 (35-60%) 2209.1 (60-77%) 8767.4 (77-83%)	0-83%	Nonlinear	–	5000 cycles (60%)	Wearable, full-spectrum, human health and motion monitoring systems	(Shi et al., 2018c)
			High-crack-density vertical graphene nanowalls	72 (20%) 22,000 (100%)	0-100%	Nonlinear	0-3 kHz	1000 cycles (40%)	Wearable devices for human motion, pulse, and sound timbre detection	(Deng et al., 2019)
			Hydrophobic polyimide nanofiber/MXene composite aerogel	1.67	0.5–90%	Nonlinear		1000 cycles (50%) 200 cycles (80%)	Human body motion and physical signals Detection	(Liu et al., 2021)
		Pressure	MXene/cotton fabric	5.30, 2.27, 0.57, 0.08 kPa^{-1} for the pressure ranges of 0–1.30, 1.30–10.25, 10.25–40.73, 40.73–160 kPa	0-160 kPa	Nonlinear	–	1000 cycles (80kPa)>	Human health signal detection and advanced flexible intelligent E-skin	(Zheng et al., 2021b)
			MXene/protein nanocomposites	298.4, 171.9 kPa^{-1} for 1.4–15.7, 15.7–39.3 kPa	0.089–39.3 kPa	Nonlinear	–	10,000 cycles (0-7142 Pa)	Degradable devices, smart electronic skins, human motion detection, and disease diagnosis	(Chao et al., 2021)
			MXene-coated carboxylated carbon nanotubes (C-CNTs)/ carboxymethyl chitosan (CCS) aerogel	3.84, 0.18 kPa^{-1} for 0–12.4, 32.8–80.9 kPa	0-80.9 kPa	Nonlinear	0.13 −0.25Hz	1000 cycles (0-30%)	Electronic skin, wearable device, intelligent medical monitor and other electronics under watery and sweaty environments	(Yang et al., 2021)

(*Continued on next page*)

Table 1. *Continued*

Transduction principles	Advantages/ Disadvantages	Sensed mechanical type	Key materials	Sensitivity (GF)	Range	Linearity	Vibration response	Cyclic stability	Application	Ref.
Capacitance	√ High sensitivity √ Temperature independent √ Well established fabrication technique √ Low power consumption × Highly susceptible to parasitic influence and electromagnetic interference × Complex circuitry ×Crosstalk between sensing unit	Strain	MXene-coated cellulose yarns	6.02	0-20%	Linear	–	2000 cycles (0-14%)	Textile-based electronics, finger touch detection	(Uzun et al., 2019)
			Vertical graphene Electrode	0.97	0-80%	Linear	–	1000 cycles (0-80%)	Detecting human physiological signals and applications in e-skin and robotics	(Deng et al., 2020)
		Pressure	MXene nanosheets based iontronic> sensor	S_{min}>200 kPa^{-1}, S_{max}>45,000 kPa^{-1}	0-1.4 MPa	Nonlinear	–	10,000 cycles (0-510 kPa)	Human activity and robotic grasping monitoring	(Gao et al., 2021)
			MXene nanosheet dielectric with a 3D network electrode	10.2 kPa^{-1} (0–8.6 kPa); 3.65 kPa^{-1} (8.6–100 kPa)	0-100 kPa	Nonlinear	–	20,000 cycles (0-12 kPa)	Compact wearable and tiny electronics	(Zhang et al., 2021)
			MXene/PVDF-TrFE composite nanofibrous scaffolds as a dielectric layer	0.51 kPa^{-1}	0–400 kPa	Nonlinear	–	10,000 cycles (0-167 kPa)	Human physiology monitoring and wearable healthcare Devices	(Sharma et al., 2020)
			MXene/Ag NWs composite electrodes	3.65–418.2 MPa^{-1}	0-600 kPa	Nonlinear	–	1800 cycles (0-40 kPa)	Healthcare, soft robots, human–machine interaction, and wearable devices	(He et al., 2021)
Piezoelectricity	√ High sensitivity √ Good dynamic response √ Low-power-consumption or self-power ability × Not suitable for static sensing × Susceptibility to temperature × Drift of sensor output over time	Strain	2D structures lead (II) iodide (PbI_2) nanosheets	10-25 (0.339%)	0.137%–0.339%	Approximately linear	–	4500 cycles (0.339%, 5 Hz)	Wearable electronics and distributed sensing networks	(Song et al., 2018)
			Single-atomic-layer MoS_2	760 (0.53%)	0.21–0.64%	Nonlinear	–	9000 cycles (0.43%, 0.5 Hz)	Wearable technology, pervasive computing and implanted devices	(Wu et al., 2014)
		Pressure	Large-scale sputtered, asymmetric 2D MoS_2	262 mV/kPa	1-5 kPa	Linear	–	>1000 s (5 kPa)	Emerging bioinspired robotics and biomedical applications	(Choi et al., 2021)
			CVD Grown WS_2	19.8mV/kPa 0.756pA/kPa	1-5 kPa	Linear	–	–	Stretchable or wearable electronics	(Kim et al., 2020)

(*Continued on next page*)

Table 1. ***Continued***

Transduction principles	Advantages/ Disadvantages	Sensed mechanical type	Key materials	Sensitivity (GF)	Range	Linearity	Vibration response	Cyclic stability	Application	Ref.
Triboelectricity	√ High sensitivity √stronger output signal √ easy structures and extensive material selection √great efficiency at low operating frequencies × Not suitable for static sensing ×not durable	Strain	1D silver nanowires (AgNWs) network wrapped with 2D metallic MoS_2 nanosheets	215.4	70%	Nonlinear	1-30 Hz (10 N)	1000 cycles (0-30%)	Human-motion strain sensor and self-powered wind speed sensor	(Lan et al., 2019)
		Pressure	Wrinkled PDMS/ MXene composite Films	0.18 V/Pa (10–80 Pa 0.06 V/Pa (80–800 Pa)	10-800 Pa	Nonlinear	–	10,000 cycles (800 Pa)	Monitoring human physiological signal and imitating human touch sensation	(Cai et al., 2021)

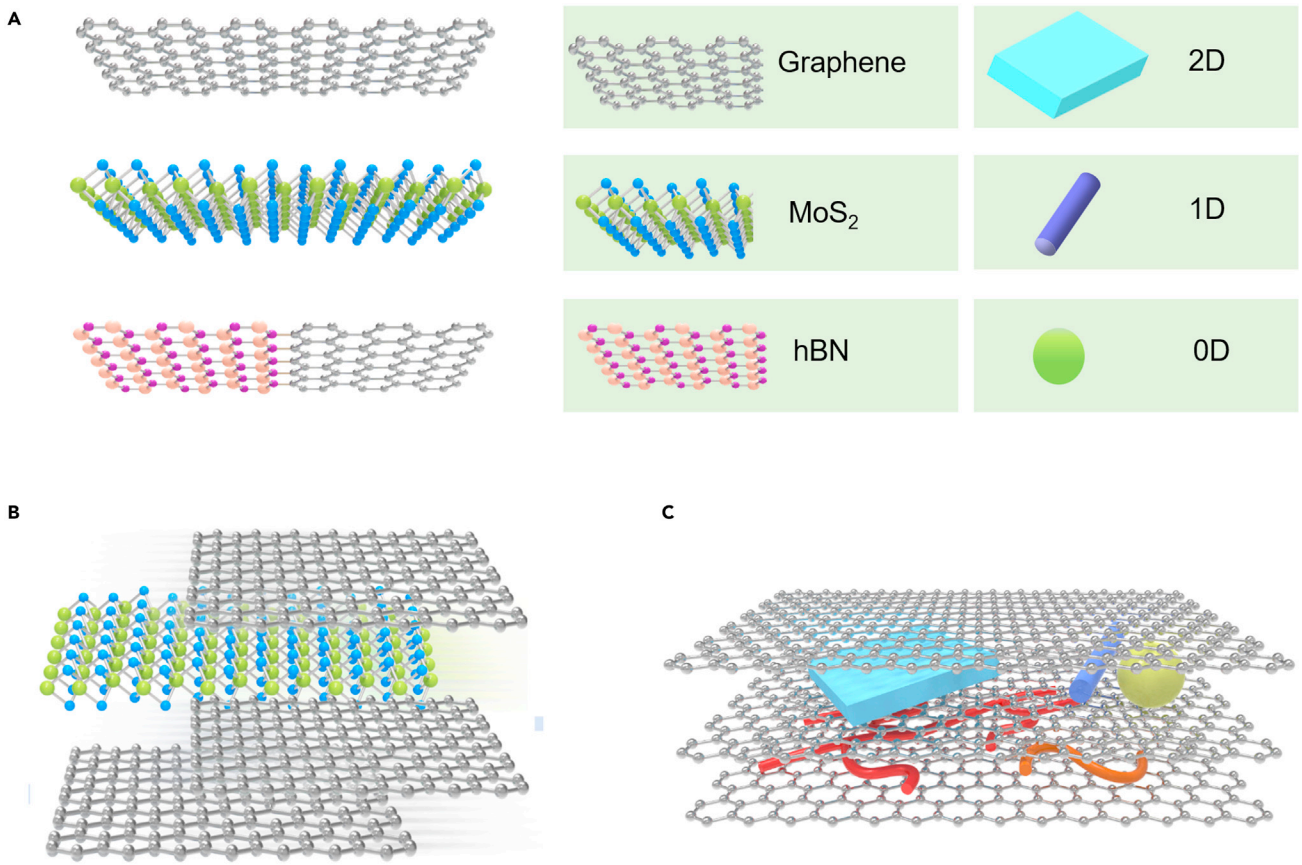

Figure 2. 2D geometries

(A–C) (A) Lateral 2D crystal structures; (B) Vertical 2D crystal structures; (C) Heterogeneously designed 2D crystal composite structures.

et al., 2016). Many physical properties of a vertical stack are sensitive to the applied in-plane and out-of-plane loadings. The former can activate the straining or shearing of the layers (Oviedo et al., 2014; Wang et al., 2017a), and the latter can often alter its atomic layer spacing, thus either in-plane transport for conducting 2D crystals or out-of-plane tunneling through spacing interfaces could be modulated (Li et al., 2016a; Ren et al., 2019; Wang et al., 2015b). The piezoresistive performance of 2D crystals in a vertical stack also depends on the mechanical properties and behaviors of each layer and the vdW interfaces between layers (particularly interfacial shear and adhesion). In a vertical stack, layers are held together by vdW interactions. Compared with interfaces between a 2D crystal and a regular substrate, the 2D-2D interfaces involve much richer nano/microscale subtleties regarding topological structures and interfacial interactions due to the atomic proximity. Here, we firstly discuss the shear strength and adhesion of 2D crystal interfaces as a quantitative understanding of them would be highly beneficial to the design of 2D crystal-based mechanical sensing systems. We refer to more comprehensive reviews (Liechti, 2019) that contain in-depth discussions on the multi-scale traction-separation behaviors of 2D interfaces.

Shear

Very recently, experimental advances have enabled the characterization of the fundamental interlayer shear of 2D materials in multilayer stacked systems. For example, the interlayer shear strength in the bilayer graphene interface has been estimated to be ~0.04 MPa by Raman spectroscopy–combined pressurized bubbles devices (bulge test) (Wang et al., 2017a), which is ~40 times weaker than that at the graphene-SiO_2 interfaces estimated via the same methodology. *In-situ* transmission electron microscopy (TEM) characterization of interlayer sliding in the cross-section view of MoS_2 suggested an interlayer shear strength of ~25.3 MPa according to a nano-indentation force sensor (Oviedo et al., 2014). On the other hand, the

interfacial shear strength between 2D materials and regular (3D) substrates (e.g., elastomers) deserves attention. Based on *in-situ* mappings of the Raman band shift, the interfacial shear strength between monolayer graphene and polyethylene terephthalate (PET) substrate was estimated with the aid of a nonlinear shear-lag model, ranging from 0.46 to 0.69 MPa (Jiang et al., 2014). Note that the concept of the shear-lag model may be extended to 2D-2D interfaces with a registry-dependent interlayer interaction potential (Kumar et al., 2016). A critical prediction of such modeling that may be useful for the design of 2D material sensors is the maximal strain the vdW interface can transfer to 2D materials. At 2D-3D interfaces, the maximal strain is approximately determined by $\frac{\tau_c L}{2E_{2D}}$ according to the shear-lag model, where τ_c is the interfacial shear strength, L is the size of the 2D flakes, and E_{2D} is the in-plane stiffness of the 2D flake (Dai et al., 2019b). The large stiffness of 2D materials, together with the relatively weak interfacial shear strength, limits the strain transfer efficiency at 2D material interfaces. Similar scenarios happen to 2D-2D interfaces with even weaker interlayer shear resistance, which could be described by a modified shear-lag mode. In general, one may expect that the interfacial sliding between 2D layers instead of actual lattice deformation occurs when 2D devices undergo strain levels greater than ~1% (Dai et al., 2019b; Gong et al., 2010; Jiang et al., 2014; Kumar et al., 2016). According to the simple shear-lag theory (Dai et al., 2019b), increasing the lateral size of 2D layers (Xu et al., 2016) and reinforcing the interfacial shear strength either physically or chemically (Wang et al., 2017b) would maximize the interface-transferred strain.

Adhesion

The interfacial adhesion between 2D crystals and substrates has been a significant concern when considering their integration into mechanical sensing devices. The energetical competition between adhesion and elasticity selects a wide range of mechanical deformation modes and characteristics, including the cleavage of atomic layers upon shear load (Tang et al., 2014; Wang et al., 2015a) and the delamination (or, more broadly, out-of-plane instabilities) of substrate-supported 2D materials (Brennan et al., 2015; Deng and Berry, 2016; Lanza et al., 2013; Pan et al., 2014). From the perspective of device manufacturing, the adhesion between 2D materials and their neighbors (including polymeric substrates, metallic interconnects, encapsulation layers, and other elements of a complete system) governs the mechanical integrity of the device upon thermal and mechanical loadings (Brennan et al., 2015) as well as the conformability of the device to the targets (e.g., epidermal skin). A theoretical framework for estimating adhesion work for various 2D material interfaces according to the experimentally measured blister profiles has been developed (Dai et al., 2018; Sanchez et al., 2018). The values of adhesion energy of various 2D interfaces range from tens to hundreds of mJ m^{-2} (Sanchez et al., 2018).

Besides shear, the adhesion control may provide a convenient and gentle way to modulate the performance of 2D material devices. Optimizing the surface adhesion of substrates would, in turn, reduce the shear force between 2D stacking layers (Choi et al., 2011) due to the suppressed puckering phenomenon (Lanza et al., 2013), affecting the interface-related sliding and cracking behavior. Increasing the interfacial resistance through the assembly of surfactant molecules between 2D flakes or introducing more flake-flake interface by reducing flake size could provide additional routes to increase the sensor sensitivity (Chen et al., 2016b). More details about the shear and adhesion mechanics of 2D materials and related influencing factors are recommended to other references (Akinwande et al., 2017; Androulidakis et al., 2018; Dai et al., 2019b; Gao et al., 2015).

Mechanoelectrical coupling properties

Different piezoresistive behaviors may occur depending on the interface-related sliding and cracking behaviors. As stated before, for vertical stacks of 2D layers, interfacial sliding between 2D layers instead of actual lattice deformation may occur when 2D material devices undergo strain levels greater than ~1%. In such case, 2D layers stacked on top of each other look like "fish-scales", and the slippage between 2D layers would change the overlapping area between adjacent 2D flakes during stretching and releasing, thus producing interlayer resistance changes (Kim et al., 2011c). The interlayer resistance is inversely proportional to the overlap area and is commonly more dominant than the intralayer resistance of 2D flake (Wang et al., 2015b). Conductivity change governed by the slippage between neighboring flakes proposes a direct strategy to achieve higher sensitivity for mechanical sensors than that governed by the lattice deformation itself. Many groups utilized this mechanism to obtain strain sensors with high gauge factors (Jing et al., 2013; Li et al., 2012b). Modeling of percolation through a 2D flake network under strain has been established by displacing the flakes according to the elongation of the entire device and recalculating the corresponding equivalent network resistance as shown in Figure 3A (Hempel et al., 2012). As the strain

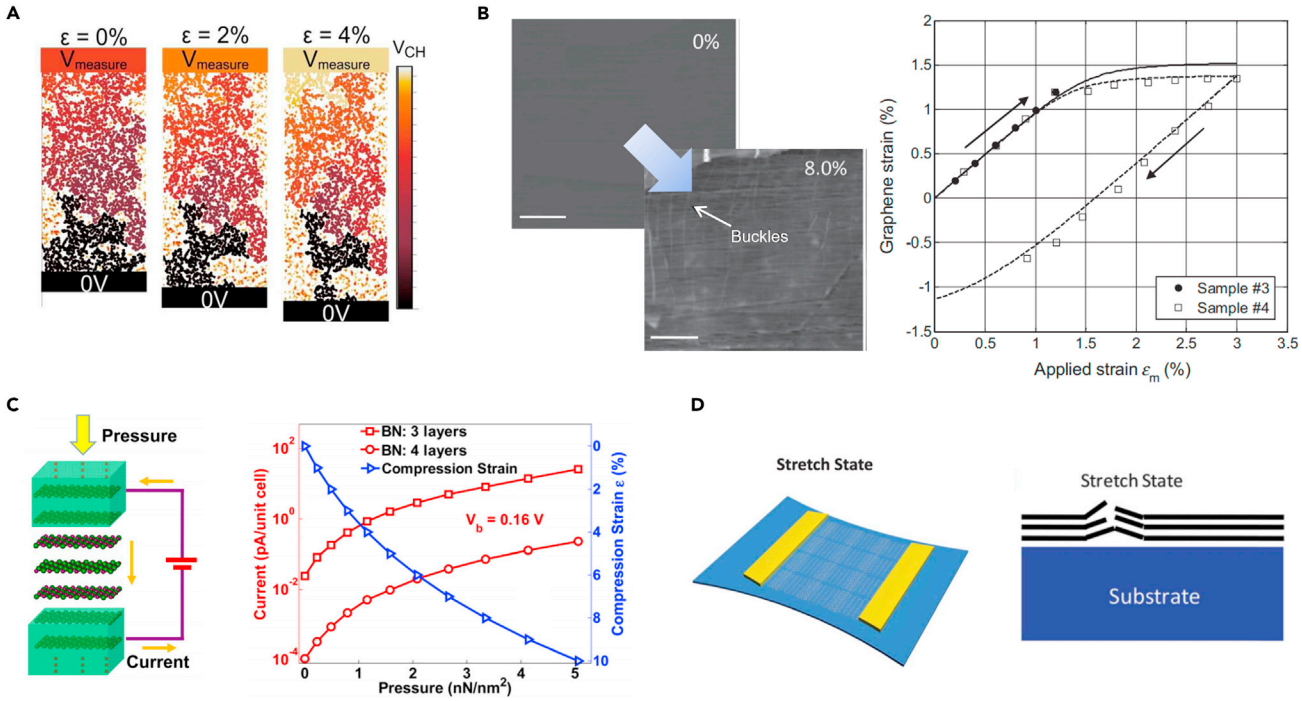

Figure 3. Mechanoelectrical coupling mechanisms related to the interface-related sliding and cracking behaviors

(A–D) (A) Slippage induced conductivity change between neighboring flakes; (B) Slippage induced buckling for graphene film after stretch and release (left), and the center strain in graphene during loading and unloading (right) (scale bars: 10 μm); (C) A tunneling pressure sensor based on graphene/h-BN/graphene sandwich structure (left) and corresponding measurement results (right); (D) A graphene-on-PET strain sensor based on fractured structures. Adapted from Refs. [(Hempel et al., 2012) (Jiang et al., 2014) (Xu et al., 2011), (Tian et al., 2014)].

increases, the overlap area between 2D flakes gradually decreases, and then some physical interconnection loss (namely, cracks) occurs, leading to a decrease in the conductive path, which in turn influences the electrical characteristics. A modified Voronoi polycrystalline micromechanical bio-inspired model has also been established to further reveal the influences of overlapping width, strip size, Poisson's ratio of the substrate material, size effect, interfacial resistance, etc., on the strain sensing properties of devices based on such "fish-scale" like structure (Wang et al., 2015b).

In the second case, sliding sometimes occurs preferentially at the 2D flake/substrate interface when a mechanical load is applied. Such slippage leads to buckle delamination or wrinkles of 2D materials when the substrate is unloaded (Deng and Berry, 2016; Yang et al., 2017b). For example, a detailed investigation of the interfacial sliding and buckling of monolayer graphene on PET substrate has been reported as shown in Figure 3B (Jiang et al., 2014). As the PET substrate was stretched, the interfacial stress transfer led to tension in graphene, and the critical strain for onset of interfacial sliding was found to be ~0.3%. The maximum strain that could be transferred to graphene ranged from 1.2% to 1.6%, depending on the interfacial shear strength and graphene size. The retraction of the substrate would impose a compression to graphene while such compression was usually released by the formation of buckling ridges (Xu et al., 2015). These corrugations induce additional scattering for charge carries (Zhu et al., 2012) and increase the resistance (Wang et al., 2011). Moreover, these buckles and wrinkles play important roles in determining the resistance change during stretching (Wang et al., 2011). For example, buckled graphene ribbons were fabricated after being transferred onto a pre-strained polydimethylsiloxane (PDMS) substrate (Wang et al., 2011). The sheet resistance decreased linearly from 5.9 to 3.6 kΩ due to the flattening of the buckles when the substrate was subjected to a strain of up to 20%. By contrast, a buckled nanographene film on PDMS prepared via a similar process showed an opposite trend (gauge factor: ~0.55 under tensile strains) (Wang et al., 2011). For the nanographene film, the buckling resulted in a more compact stacking between graphene domains. The stretching process would increase the sheet resistance due to the reduced electrical percolation pathways in the film.

In the third case where a 2D material film comprises isolated islands or cut-through fractures, the tunneling effect contributes dominantly to the piezoresistive properties, leading to extremely high sensitivity. Isolated islands of graphene could be developed via plasma-enhanced CVD (Zhao et al., 2015) or solution self-assembly (Li et al., 2016b) method. The current flow from one isolated graphene flake to another due to the tunneling effect. In devices designed this way, the resistance changes drastically with the distance. Experimentally, a substantial resistance change has been observed in a quasi-continuous graphene film under the stretching, providing the strain sensor with a super GF of more than 500 under 1% strain (Li et al., 2016b). A tunneling pressure sensor consisting of h-BN sandwiched by graphene has been demonstrated, whereas the tunneling current exhibited a positive correlation to pressure, as shown in Figure 3C (Xu et al., 2011). It has also been reported that cut-through fracture occurred in 2D layered material film where vertically stacked 2D crystals were regarded as brittle conductive materials as a whole (Chen et al., 2019; Tian et al., 2014; Xu et al., 2019). The geometry of cut-through fracture in a 2D layered material is closely associated with film/substrate interaction. The strain localization could be from the imperfection of geometry (including ridges, free edges, interruptions of the coating, irregular substrate, and necking of thermoplastic polymer substrate) on a localized region of the film as well as from non-uniform interfacial bonding. Then the concentrated stress causes the delamination of the film-substrate interface and the formation of micro-cracks on the film. Micro-cracks might propagate and develop into channel cracks (or cut-through fracture) traversing the entire width of the film, as shown in Figure 3D. The formation of cut-through fracture would make the current conducted by the tunneling effect through pairs of relatively close steps on opposite edges of fracture. The device resistance upon a tiny strain exhibits a sudden jump (Dinh et al., 2019).

In fact, the above three cases are not completely separated; the actual working principles may involve different cases in different loading stages (Dinh et al., 2019; Liu et al., 2015). For example, wrinkles or buckles may be first flattened when 2D layered material film is subjected to small strains. The resistance of the sensing film in this region changes slowly. As the stretch further increases, sliding effect between adjacent 2D flakes dominates the electron transport and the total resistance shows a more pronounced response to the applied strain. Upon larger strain, adjacent 2D flakes lose physical contact, in accompany with the growth and propagation of cracks, which finally makes current flow between the crack edges possible only *via* electron tunneling.

Heterogeneously designed 2D crystal composite structures

The modification of functional components attached to the 2D crystal can adjust its surface and interface chemistry and facilitate its integration with other materials to form heterogeneous composite structures. From the modification of 2D crystals to the construction of unique macroscopic and microscopic structures, the so-called synergistic effect of different properties of each component material is frequently mentioned in the literature that helps to construct more magic stimulus-responsive smart materials. Mechanical sensors based on different composite structures of 0D-2D, 1D-2D, 2D-2D, 3D-2D, 0D-1D-2D, and 0D-2D-3D, have been reported. The following are a few representative examples to discuss the effect of adding 0D, 1D, and 3D components on the mechanical sensing properties of 2D materials.

For example, the nacres have outstanding mechanical properties combining high strength and toughness, which is due in part to its hierarchical layered architecture with rich interfacial interactions. Inspired from the nacre, a strain sensor based on the nacre-mimetic microscale "brick-and-mortar" architecture has been reported, in which 2D titanium carbide (MXene) $Ti_3C_2T_x$/1D silver nanowire functions as "brick" and poly (dopamine)/Ni^{2+} functions as "mortar" as shown in Figure 4A (Shi et al., 2018c). The synergistic behavior of the "brick" and "mortar" can control the generation of cracks to achieve high sensitivity, but can also dissipate a large amount of loading energy, thereby promoting the stepwise propagation of cracks during stretching to achieve large stretchability at the same time.

Another strain sensor based on the 0D-1D-2D ternary nanocomposite shows high sensitivity with a GF of ~2390 at 62% working strain. The 0-D fullerene has lubricating property and induces interlayer slippage between adjacent 2D sheets to accommodate applied stress as shown in Figure 4B. The 2D graphene generates many cracks through interlayer slippage to ensure a large resistance change in the entire working strain range. The highly conductive 1D silver nanowire (AgNW) provides a conductive path to connect the adjacent 2D sheets during the crack propagation, further expanding the working range of the device. Such 0D-1D-2D composite structure renders the strain sensor with high comprehensive performance and be applicable to full-spectrum human motion detection (Shi et al., 2018b).

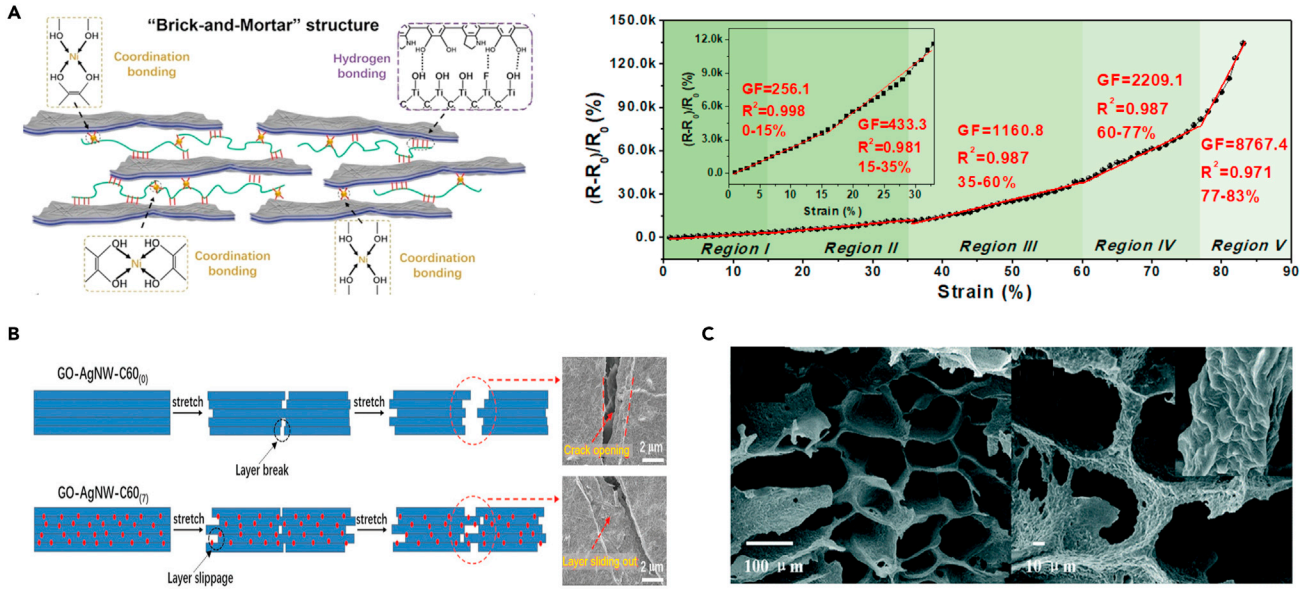

Figure 4. Heterogeneous composite structures based on 2D crystals

(A–C) (A) $Ti_3C_2T_x$-AgNW-PDA/Ni^{2+} sensor with a "brick-and-mortar" structure, and the corresponding electrical response under different strain; (B) Schematic illustration of sensing mechanism for GO-AgNW sensing film versus GO-AgNW-C60 sensing films; (C) Morphology of the graphene/TPU foam. Adapted from Refs. [(Shi et al., 2018c) (Shi et al., 2018b), (Liu et al., 2017a)].

It is noteworthy that metallic 2D materials are often used as conductive nanofillers for 3D elastic polymers such as natural rubber and TPU to form conductive skeletons (Lu et al., 2019; Raju et al., 2014). One example is the graphene/polyurethane (TPU) composite foam structure (Figure 4C) with large porosity, low mass density, and good electrical conductivity, which is used as sensing materials to detect tensile or compressive strains (Liu et al., 2017a).TPU here functions as structural support material to ensure the robust structure of the foam, endowing the device with ultra-high compressibility while showing good recoverability and reproducibility after stable cyclic loading. When the force load is applied, the spacing and overlapping contact areas between adjacent 2D sheets changes, thereby generating an electrical signal. Compared with 1D conductive fillers (e.g., CNTs), 2D fillers are expected to exhibit higher strain or pressure sensitivity due to their larger contact area. Therefore, the force-sensitive characteristics of 2D nanosheets/3D polymer nanocomposites have attracted extensive attention, and many performance modulating strategies are introduced in the following.

The piezoresistivity of 2D nanosheets/3D polymer nanocomposites have been observed and two possible mechanisms have been proposed: (1) strain-induced break-up/reforming of the percolating pathway and (2) the change of sheet-to-sheet resistance (or electron tunneling that varies dramatically as a function of the sheet distance). To achieve high-performance mechanical sensors, the concentration of 2D sheets is preferred to be around the percolation threshold where break-up and reforming of the percolating pathway would dominate piezoresistive characteristics. The addition of 2D materials in polymer to form conductive elastomer has been exploited to develop the strain/pressure sensing devices. For example, composites consisting of graphene, poly (acrylic acid), and amorphous calcium carbonate have been fabricated into stretchable strain sensors of various structures (sandwich structures, fibrous structures, self-supporting structures, etc.) (Lin et al., 2019). The addition of graphene could decrease the value of tan δ of the nanocomposite and thus enhance its elastic recovery performance. The developed sensor could withstand high elastic deformation (up to 500%) and be suitable for detecting various biological signals, including crawling, undulatory locomotion, and human body motion. Besides, the introduction of porous or foam structures into these composite materials, such as graphene porous network embedded in PDMS, have demonstrated improved sensitivity and wider sensing range for detecting mechanical deformation (Pang et al., 2016). It is noteworthy that embedding graphene in highly viscoelastic polymer matrices has displayed unusual mechanoelectrical behavior as the connectivity and mobility of the nanosheets are closely associated with the low-viscosity property of the substrate (Boland et al., 2016). These

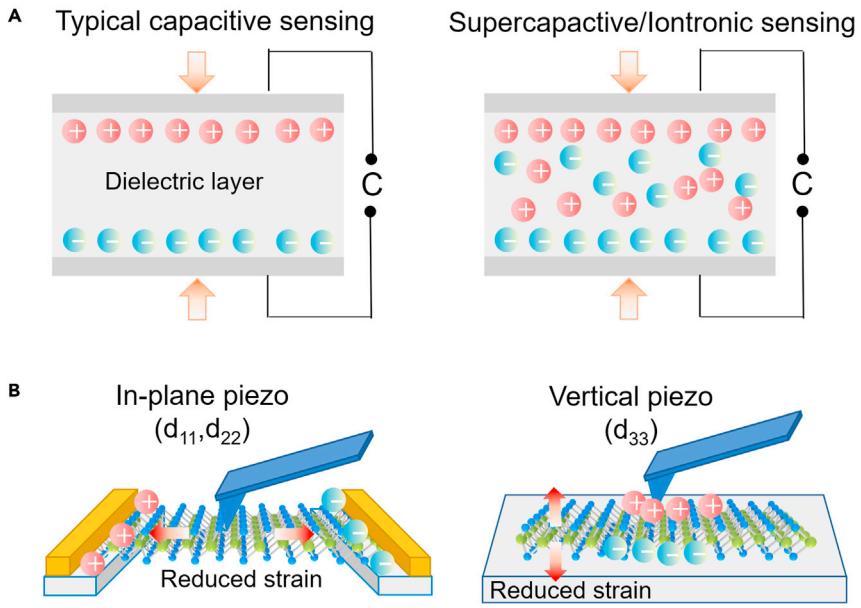

Figure 5. Capacitive and piezoelectric principles

(A and B) (A) Typical capacitive sensing and supercapacitive/iontronic sensing; (B) Typical piezoelectric d_{11} and d_{33} working modes.

nanocomposites have potential in highly sensitive mechanical sensors due to their high gauge factors (>500), which have been used to measure pulse, blood pressure, and even the tiny vibration associated with the footsteps of a small spider. Some new phenomena, such as post-deformation temporal relaxation of electrical resistance and nonmonotonic changes in resistivity with strain, have also been observed in these viscoelastic 2D-polymer nanocomposites (Boland et al., 2016).

Capacitive, piezoelectric and triboelectric principles

Capacitive principle

2D materials can be used as electrodes or dielectric layer materials for capacitive sensors. If the fringe effect is neglected, one of the simplest models is the parallel plate capacitor. When the force is loaded, the capacitance (C) is proportional to the electrode area (A), the dielectric constant (ε) and the reciprocal of the distance (d) between the electrodes, which converts the perceived mechanical changes into electrical signals (Chen et al., 2016a; Yang et al., 2019a). For the sensor design, the applied force usually causes the elastic structural material to shift, resulting in the changes of the variable d or A, so that the force to be measured can be deduced inversely. For example, graphene with high conductivity was used as the electrodes, and 3D ultra-light porous GO foam with good elastic properties and a high relative dielectric constant was used as the dielectric layer to construct a capacitive pressure sensor. When the pressure was applied, the distance d, i.e., the thickness of the GO foam, between the electrodes varied quickly, allowing the detection of subtle pressure change as low as 0.24 Pa (Wan et al., 2017). Compared with the piezoresistive principle, capacitive sensors are easy to achieve better frequency response, less temperature influence and less power consumption. However, in order to prevent electrical breakdown and pull-in effects, the distance d is usually greater than 1 μm, and most dielectric materials have limited permittivity, so that the capacitance is only tens to hundreds of pF cm^{-2} (Chang et al., 2021; Mansfeld et al., 2010; Yang and Suo, 2018). This value is equivalent to the parasitic influence along the transmission line and the electromagnetic noise from the surrounding environment, which make capacitive sensors quite sensitive to parasitic effects and have relatively low signal-to-noise ratio.

To address above issues, a brand-new mechanical sensing mode, called interfacial supercapacitive sensing or iontronic sensing, has been proposed (Chang et al., 2021). By using the supercapacitor characteristics of the electric double layer at the elastic dielectric/electrode interface, mechanical deformation can be detected, as shown in Figure 5A. Compared with traditional capacitors, this new interfacial supercapacitive sensing method demonstrated an ultra-high unit-area capacitance (UAC). The capacitance value is about a few μF cm^{-2} in the sub-MHz spectrum region, which is 1000 times larger than that of traditional parallel

plate capacitive sensors (Chang et al., 2021; Nie et al., 2012; Zhu et al., 2021). This sensing method generally has comprehensive advantages such as ultra-high device sensitivity, high noise immunity, and thin and flexible device architecture. The huge specific surface area, abundant pore structure and flexible surface chemical modification of 2D materials make them very suitable as electrode for iontronic sensing. For example, MXene ($Ti_3C_2T_x$) with high capacitance characteristics was used to construct capacitive electrodes. The accessible surface area of MXene increases and the ion transmission path is shortened when stressed, making the sensor exhibit an unprecedented ultra-high sensitivity exceeding 46,730 kPa^{-1} and an ultra-wide sensing range of 1.4 MPa (Gao et al., 2021). Such devices showed good prospects in the fields of robot intelligence, electronic skin, and wearable health. For more information, please refer to other review literatures (Chang et al., 2021).

Piezoelectric and triboelectric principles

In addition to the piezoresistive and capacitive principles, self-powered sensors that do not require external electrical energy have received widespread attention in recent years, with piezoelectric and triboelectric types as typical representatives. The piezoelectric effect means that when a material is deformed by an external force in a certain direction, polarization will occur inside it, and meanwhile, positive and negative charges will appear on its two opposite surfaces (Mahapatra et al., 2021). A range of 2D materials with non-centrosymmetric structures have been theoretically predicted and/or experimentally confirmed as piezoelectric or ferroelectric materials (Cui et al., 2018; Duerloo et al., 2012; Fei et al., 2015, 2016; Hu and Dong, 2016), including MoS_2, $MoSe_2$, WS_2, WSe_2, GeSe, and SnS, *etc.* The use of strong, flexible, ultrathin piezoelectrics of 2D layered materials, compared to traditional piezoelectric ceramics, is more suitable for some important applications, such as artificial intelligent interface electronics and flexible/wearable devices (Dai et al., 2019a). There are mainly two working modes: in-plane piezoelectric mode (d_{11} and d_{22}) and vertical piezoelectric mode (d_{33}) (Qi et al., 2015; Wang et al., 2016; Wu et al., 2014; Zheng et al., 2021a; Zhu et al., 2015). In the d_{11} and d_{22} working modes, the piezoelectric material is subjected to tensile or compressive stress in the in-plane direction. The material polarization and the generated electric field are also along the same direction as the applied stress. When the d_{33} working mode is adopted, the piezoelectric material is subjected to tensile or compressive stress in the out-of-plane direction (*i.e.*, the vertical direction). The generated electric field is also along the vertical direction. A schematic diagram of the corresponding working mode is shown in Figure 5B.

Recent experiments have revealed that MoS_2 containing an odd number of atomic layers shows an in-plane piezoelectric effect and produces oscillating piezoelectric voltage and current outputs (Zhu et al., 2015). For a free-standing single layer of MoS_2, its single-layer structure has a great in-plane piezoelectric coefficient of 2.9×10^{-10} $C \cdot m^{-1}$, which is even larger than some traditional bulk piezoelectric materials (Zhu et al., 2015). However, for most vdWs layered piezoelectric materials, their in-plane piezoelectricity decreases significantly as the number of atomic layers increases, because the reverse polarization direction between adjacent layers causes polarization cancellation (Dai et al., 2019a; Wu et al., 2014; Zhu et al., 2015). Therefore, their exceedingly small effective volume leads to insufficient piezoelectric outputs, which is difficult to meet the high responsivity requirements of actual device applications. In order to overcome the above-mentioned bottleneck, adjacent 2D layers are expected to have the same polarization direction. Some 2D vdWs piezoelectric materials have been reported, which showed in-plane piezoelectric coefficients increasing with the number of layers due to the same polarization orientation between adjacent monolayers. Therefore, by using a multilayer structure, a large piezoelectric output signal can be provided. For example, the adjacent monolayers of α-In_2Se_3 have the same polarization direction, and a 7-layer α-In_2Se_3 device shows a piezoelectric output with a voltage responsivity of 0.363 V and a current responsivity of 598 pA under 1% strain, which has been used for real-time health monitoring (Dai et al., 2019a).

Some 2D materials show strong out-of-plane piezoelectric properties, which are more suitable for detecting vertical pressure stress relative to the in-plane direction. For example, an ultra-thin CdS film with a thickness on the atomic scale (three to five spatial lattices) shows a vertical piezoelectric coefficient (d_{33}) as high as 33 $pm \cdot V^{-1}$, which is three times larger than that of bulk CdS (Wang et al., 2016). For more introduction on the piezoelectric properties of 2D materials, please refer to other review articles (Jiang et al., 2020; Zheng et al., 2021a). In addition, although graphene does not have piezoelectric effect, it is suitable to function as a reinforcement or electrode for piezoelectric materials (Chen et al., 2017b). Generally, the piezoelectric signal sensed by the piezoelectric effect is an instantaneous signal, which is only suitable for detecting dynamically changing force stimulation, thus it is difficult to realize steady-state monitoring. To solve the

problem, a pressure sensor based on the composite heterostructures of graphene and piezoelectric nanowires has been proposed, in which strain-induced polarization charges in piezoelectric nanowires cause the change of carrier scattering in graphene, thereby obtaining the pressure sensor to measure static pressure with high sensitivity and fast response time (Chen et al., 2017c).

The triboelectric effect is a phenomenon in which two materials with different properties are charged through friction or contact. The frictional charge on the surface of the dielectric is changed by force stimulation, thereby realizing mechanical signal detection (Garcia et al., 2018; Tao et al., 2019; Xiang et al., 2017). Generally, the performance of sensors based on triboelectric effect is related to the magnitude of external stress and frequency of force stimulation. The mechanical sensors prepared by the triboelectric effect also have the self-power capability, and compared with the piezoelectric effect, their output voltage amplitudes are higher, becoming suitable for constructing ultra-thin on-skin mechanical sensors. For example, graphene was used as the electrode (thickness: <1 nm), PET was used as the substrate (thickness: <0.9 μm), and PDMS was used as the charged layer (thickness: < 1.5 μm) to prepare a pressure sensor that could be directly attached to human skin (Chu et al., 2016). Electricity was generated by contact with clothes or human body to detect a variety of human motions. In short, the flexible properties of 2D materials are combined with typical energy storage and collection methods (such as piezoelectric/triboelectric) to construct wearable devices without recharging, which has the advantage of long-term operation.

HIGH PERFORMANCE-ORIENTED STRUCTURAL DESIGN

The development of various smart structures through structural mechanics and mathematics can compensate for the limitations of the material itself and promote the functional applications of mechanical sensing. In recent years, the analysis of natural creatures as well as rational deductions has inspired many smart architectures, such as hierarchical structures (Koyama et al., 2017; Liu et al., 2017b; Tseng et al., 2017), origami or Kirigami design (Guo et al., 2016; Shyu et al., 2015; Song et al., 2014), porous structure (Kang et al., 2016; Liu et al., 2016b), interlocking structure (Pang et al., 2012a, 2012b), gradient structure (Liu et al., 2015), textile structure (Yang et al., 2018), metamaterials (Bückmann et al., 2012; Lee et al., 2012). These nature-inspired smart architectures have attracted much attention in various scientific fields because the underlying methodology constitutes an efficient path to combine multiple desirable mechanical characteristics, including lightweight, flexibility, strength, and stretchability. The high specific surface area of 2D materials and their outstanding mechanical, electrical, optical and thermal properties are attractive to "smart" materials with high-performance mechanical stimuli response.

High sensitivity

Sensitivity is one of the basic parameters that characterize the sensor performance. High sensitivity is a necessity for the accurate detection of small mechanical stimuli, such as pulse and sound waveform. Herein we mainly introduce three typical artificial structures inspired by natural organisms to develop highly sensitive wearable mechanical sensors. For example, spiders have evolved a unique sensory system that is specifically used to perceive subtle mechanical stimuli to share information with their companions or to identify nearby prey and enemies (Fratzl and Barth, 2009; Kang et al., 2014). The receptors on the spider's legs have ordered crack-type micro-nano structures, through which they respond to mechanical vibrations to stimulate sensory nerves (Fratzl and Barth, 2009). Inspired by this phenomenon, a graphene conductive thin film with spider-slit-organ-inspired microcrack structure was developed to fabricate ultrasensitive strain sensors with an ultrahigh sensitivity (GF = 8699), an ultralow detection limit (ε =0.000064%), an ultrafast response/recovery behavior, these excellent performance helps the device to perceive human voice with higher accuracy and anti-interference ability as shown in Figure 6A (Dinh et al., 2019).

The fingertip skin of the human body has a highly sensitive response to stress of different magnitudes, due to the interlocking microstructure between the dermal and epidermal layers (Park et al., 2015). Inspired by the human skin, the 2D MXene/natural microcapsule was compounded to construct a bionic interlocking structure (Figure 6B), achieving a 9.4-fold increase in pressure sensitivity (24.63 kPa^{-1}), compared to that of the planar structured counterpart (Wang et al., 2019b). Such high sensitivity allowed the device to detect many signals ranging from finger motion and human pulses to voice recognition. In addition, many kinds of natural materials have hierarchical architecture, the hierarchical micro-nano structures present in natural plants can also be used as effective soft molds. For example, by replicating the surface of the lotus leaf, the smart structures assembled by graphene nanosheets exhibited papillae morphology with nanometer/micrometer multi-level characteristics (Shi et al., 2018a). The as-fabricated piezoresistive pressure

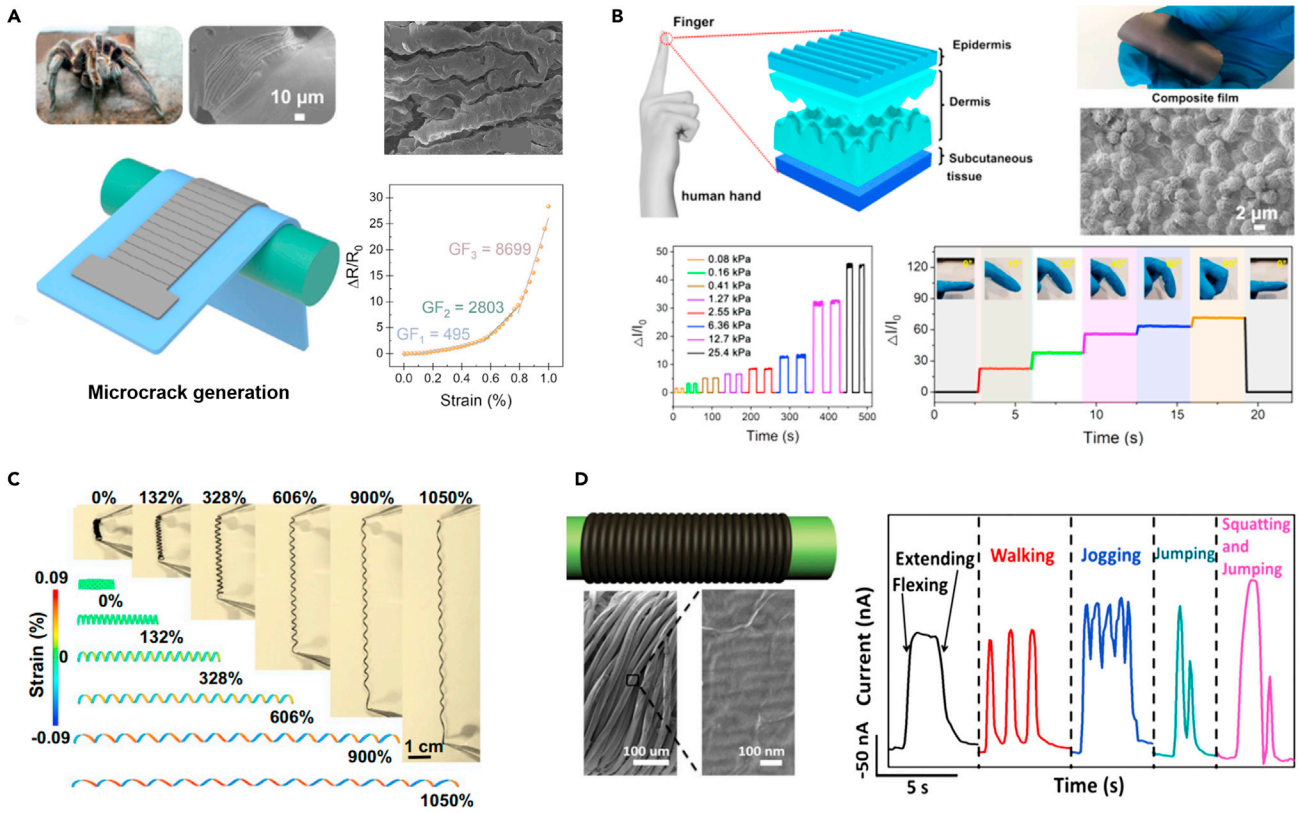

Figure 6. High performance-oriented structural designs

(A) Spider's legs inspired crack-type sensor with high sensitivity;

(B) Fingertip skin inspired pressure sensor with high sensitivity due to the interlocking microstructure;

(C) A graphene based helical spring accommodating ultra-large tensile strains (>1,000%);

(D) Double-covered yarn-shaped graphene fiber with capability to differentiate various knee-related motions, such as knee flexing/extending, walking, jogging, jumping, and squatting jumping. Adapted from Refs. [(Cheng et al., 2015) (Dinh et al., 2019) (Wang et al., 2019b), (Zhang et al., 2020)].

sensor could adapt to changing mechanical stimulation patterns and exhibited a high sensitivity of 1.2 kPa^{-1} and a wide linear range of 0–25 kPa.

In day-to-day life, the motion is rather multi-fold random, the measured sensitivity is highly dependent on the initial state of motion. In fact, only for linear sensors, there is a direct proportional relationship between sensor output and input, i.e., the GF is within the same constant value under different force loads. Therefore, in order to ensure the reliability of measured GF in different motion states, it is necessary to develop sensors that meet the requirements of high sensitivity and high linearity at the same time. However, it is currently conducive to the realization of highly sensitive structural engineering by introducing microstructures in the dielectric layer, such as microcracks, micropores, etc. The shape of the sensing element undergoes a change from homogeneous to heterogeneous during deformation, which exceeds the deformation range restricted by elastic linear mechanics, resulting in poor linearity. Therefore, nonlinearity is one of the main shortcomings of most ultra-highly sensitive strain and pressure sensors. For practical applications, it may be more practical to sacrifice a certain sensitivity coefficient to achieve a trade-off between high sensitivity and high linearity.

Large stretchability

To mimic human skin, stretchability is the basic feature for mechanical sensors to realize the function of wearability. The most popular strategy of increasing stretchability is based on the pre-strain strategy to make buckling or wavy configuration (Jones et al., 2004; Zhu and Xu, 2012). It is worth mentioning that via compressive buckling of 2D geometric micro- and nanostructures, deterministic assembly of 3D mesostructure paves new road for stretchable electronics and more details are referred to other references

(Yan et al., 2017). In addition to wavy geometry, serpentine (Xu et al., 2013), twisted (Lan et al., 2020) and helical (Won et al., 2014) structures have also been reported to endow materials with large stretch. For example, graphene nanosheets in polymer were printed into a ribbon with site-specifically varied structural alignment which spontaneously transformed into a helical spring upon stimulation, thereby accommodating ultra-large tensile strains (>1,000%) as shown in Figure 6C (Zhang et al., 2020). From the perspective of stretchable device mechanics, one primary form of stretchable design is to use island-bridge configuration (Tang and Fu, 2020; Xiao et al., 2018) in which the sensing area can be patterned into small functional islands, and the surrounding interconnection bridges are arc-shaped structures to release the stretch, thus most of the strain in the sensor area is greatly reduced.

Textile-type mechanical sensors refer to the devices based on fiber assemblies that respond to mechanical stimuli. Artificial textile is like the second layer of skin covering the human body, which is worn on people, animals or even machines. In recent years, 2D materials are processed into fibers, and then combined with textile technology to manufacture textile-type mechanical sensors (Lou et al., 2016; Shi et al., 2020; Yang et al., 2018), which wrap easily on 3D curvilinear surfaces such as human bodies. Compared with on-skin type film sensor design, the excellent structural transformation of textiles makes the fiber assembly easy to accommodate large extension, double-curvature bending and in-plane shear that usually simultaneously exist in human activities (Shi et al., 2020). For example, a composite fiber with "compression spring" structure based on graphene was fabricated, which shows a large sensing range of up to 100% strain, and an excellent life span of tens of thousands of loading cycles, as well as bending and torsion sensitivity. It was successfully worn on humans to achieve voice recognition, sleep quality assessment, pulse monitoring and exercise record (Cheng et al., 2015). Besides, 2D materials randomly incorporated into composites with other materials (such as 1D fiber (Shi et al., 2018c), 3D elastomer (Lin et al., 2019)) have also been explored to obtain mechanical sensors with large stretchability.

Dynamic and multi-axis mechanical detection

Human skins sense and distinguish various types of force stimuli, such as stretching, pressing, shearing, and twisting, and the mechanoreceptors responsible for tactile functions can respond to vibrations up to 400 Hz (Jung et al., 2019; Shao et al., 2016). In contrast to skin receptors, human ear perceives acoustic vibration in a wider range of frequencies ranging from 20 to 20,000 Hz (Jung et al., 2019), exhibiting the complexity and extraordinariness of the skin system and the auditory system. In this section, some recent progress of 2D materials-based sensors to detect dynamic mechanical stimuli are introduced. Three typical structure designs to make high-performance vibration sensors are presented. First, graphene based cellular elastomers with nano-architectured cellular network offered new dynamic mechanical properties that was drastically different from the traditional rubber-based elastomers (Qiu et al., 2016). Despite its viscoelasticity, its unique 3D nanostructured cellular network exhibited almost frequency-independent piezoresistive behavior, with a frequency response ranging from 0–2000 Hz, and ultra-low pressure of 0.082 Pa could be detected. Second, crack-type microstructure also serves as an excellent dynamic force-bearing structure with high responding speed. Different from a complete film, the high-density nano-width cracks cut the sensitive layer into many micro-nano-sized ribbons. Since the natural frequency of a ribbon is inversely proportional to its size, the natural frequency of each micro-nano-sized ribbon is high. It vibrates synchronously with high-frequency dynamic force stimulation. For example, high-crack-density vertical graphene was able to distinguish frequencies of acoustic signal higher than 2500 Hz (Deng et al., 2019).

The third typical structural design to achieve enhanced pressure sensitivity with rapid dynamic response is through incorporation of the microstructures, such as micro-pyramids. Assembling a flexible membrane composed of graphene/PDMS micro-pyramid composite with interdigitated electrodes on the opposite PET substrate created a piezoresistive pressure sensor (Yao et al., 2020). Although the viscoelasticity of PDMS led to frequency dependent piezo-sensing performance, the elasticity of graphene effectively improved the mechanical response frequency of the device, making the sensor exhibit a stable response signal to high frequency vibration of 1.5 kHz with slight distortion (Yao et al., 2020). In addition, some device designs based on piezoelectric or triboelectric principles are also suitable for vibration signal detection (Dai et al., 2019a; Park et al., 2015).

Many wearable 2D materials based mechanical sensors are reported to be sensitive to stress/strain input of multi-directions. For example, a graphene textile strain sensor exhibited relative resistance changes versus the applied strain in both the x and y direction (Yang et al., 2018). However, the signals obtained with load

from different directions are barely distinguishable. In fact, the actions of humans and robots involve forces in multiple directions, which requires sensors with multi-axis mechanical detection and discrimination capabilities. This can be achieved using three typical methods. The first method is to measure the signal response pattern from a single device; the analysis of each signal and its combined signal pattern can distinguish the force input. For example, using double-covered yarn-shaped graphene fiber, a sensor with piezoresistive response to various mechanical stimuli, including tensile strain, bending, and torsion was created (Cheng et al., 2015). The recording resistive response curve for various knee-related motions were distinctly differentiated, such as knee flexing/extending, walking, jogging, jumping, and squatting jumping as shown in Figure 6D. Such motion-related response patterns provided enough distinguishable parameters for different mechanical stimuli (Cheng et al., 2015). The second method is to estimate the mechanical input in each direction based on the unidirectional response of at least two spatially staggered stacked sensing layers. For example, three CVD graphene strain gauges with the rosette layout overcame the limits of single strain gauge which measures strain in only one direction, and showed simultaneous detection of the principal strain magnitude and direction (Bae et al., 2013). Third, sensors coupled simultaneously with multi-sensing mechanisms which provide different signal output modes including resistance, capacitance, and voltage are promising to differentiate multiple stimuli. For example, a sensor based on ferroelectric polymer composites composed of poly (vinylidene fluoride) (PVDF) and graphene was reported to perceive and discriminate static/dynamic pressure and temperature variations (Park et al., 2015). Such sensor detected static pressure, dynamic vibration and temperature via piezoresistive, piezoelectric and pyroelectric transduction principles respectively.

MULTIFUNCTION-ORIENTED STRUCTURAL DESIGN

Wearable mechanical sensors ultimately need to be applied to many aspects of daily life. In addition to the pursuit of high performance such as sensitivity and working range, another frontier is the introduction of novel material design and sensor structure design strategies to endow devices with new functions, such as biocompatibility, biodegradability, superhydrophobic, self-healing, self-powering, visualization, gas permeability, flame retardancy, and acid-alkali resistance. The continuous pursuit of high performance and multi-functional combination will greatly expand the application range of 2D materials in the field of wearable sensing.

Wearable mechanical sensors should have the biocompatibility with human body to avoid triggering an immune response. Considering the high heterogeneity of 2D crystals from various synthesis methods, the evaluation of the biocompatibility of 2D materials is still controversial (Huang et al., 2019a). One safe way to increase device biocompatibility is to choose biocompatible materials that have been tested in the market. For example, employing graphene woven fabrics with the disposable sensing contact lens, a contact lens tonometer was proposed for intraocular pressure monitoring in real time with high resolution and biocompatibility (Zhang et al., 2019). And the effectiveness of the device has been tested by an *in vitro* experiment on porcine eyes. On-skin wearable electronics continuously characterize physiological parameters to monitor human health in real time, but it is usually difficult to peel them off the skin, especially for susceptible people (such as babies and patients with skin diseases). To make them available on sensitive, fragile or even injured skin areas, skin-friendly transient epidermal electronics with biodegradability for acquiring physiological states are proposed. For example, using genetically engineered plasticized copolymer, silver nanowires and regenerated edge-decorated graphene sheets as substrates, electrodes and sensitive materials, the manufactured skin-friendly electronics measured multidimensional physiological signals, including electrocardiograms (ECG), temperature, strain, humidity, bacterial infection and so on (Zhang and Tao, 2019). Such devices can simultaneously achieve strong adhesion and easy detachment from skin, and have water-triggered, on-demand decomposition lifetime (transient capability) as shown in Figure 7A.

Super-hydrophobicity refers to an excellent water repellency, which is useful for sensors to resist potential contamination issues from the surrounding environment, thereby delaying the performance degradation during long-term use. rGO/PDMS composite films were patterned by single-step femtosecond laser direct writing, which coupled a surface morphology of lotus leaf-inspired hierarchically structure to maintain self-cleaning and water-repellent properties (Dinh et al., 2019). Meanwhile, a spider-slit-organ-inspired microcracked morphology of conductive thin film was produced under pre-stretch, which exhibited self-cleaning, ultrasensitive and anti-interference properties when attached onto skin to detect acoustic signal. Wearable sensors are easily scratched and lead to functional damage. Inspired by the ability of human skin to repair

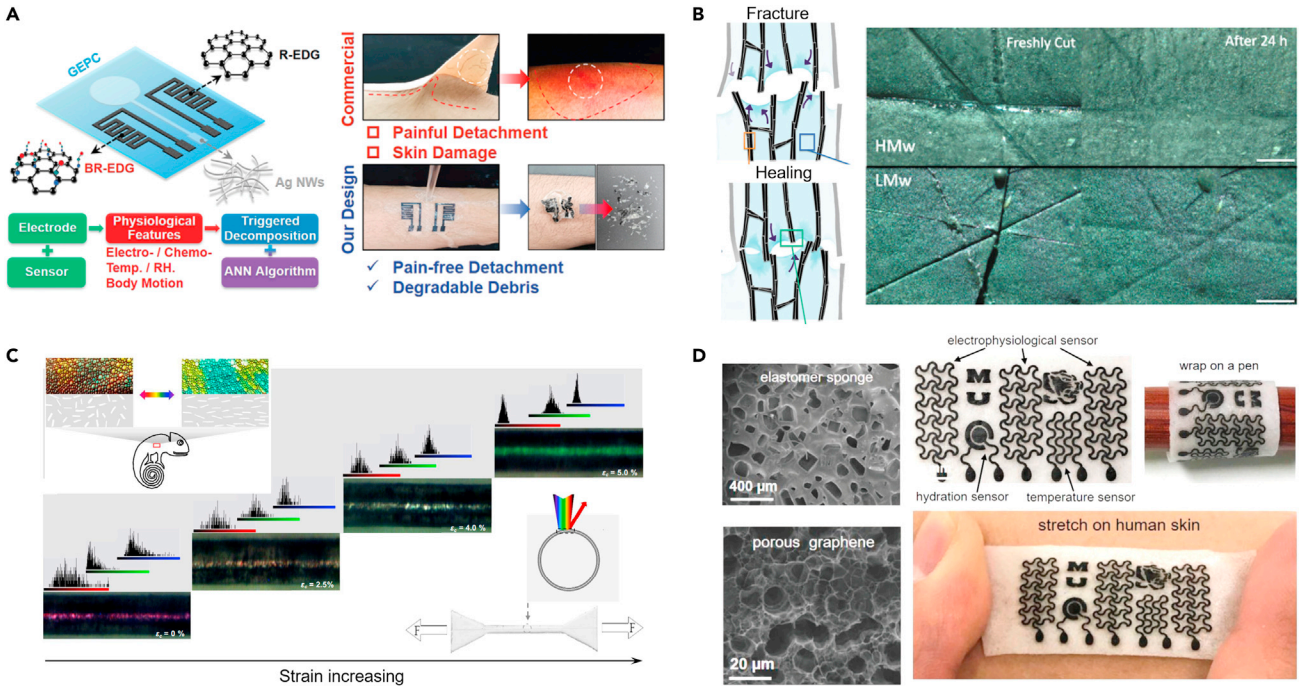

Figure 7. Multifunction-oriented structural designs

(A) Transient electronics that have abilities of strong adhesion and easy detachment from skin;
(B) Schematic and optical images of deeply scratched graphene composites during the healing process (scale bar: 1 mm);
(C) Variable structural coloration of graphene composite interphase under different strains;
(D) Graphene based sensors with good gas permeability. Adapted from Refs. [(Zhang and Tao, 2019) (D'Elia et al., 2015) (Deng et al., 2017), (Sun et al., 2018)].

itself after being mechanically damaged, in recent years, giving functional materials the ability to repair themselves has become another frontier hot spot (Chen et al., 2017a; Taylor and Panhuis, 2016). 2D materials, such as graphene, do not have self-healing ability themselves. However, the graphene based composite network constructed by combining it with self-healing polymer retained good conductivity and pressure/flexion sensitivity as shown in Figure 7B (D'Elia et al., 2015). Moreover, when damaged, the cut surfaces were reconnected autonomously to realize self-repair. Such self-repair process is repeatable and greatly extends the life of the devices.

The wearable sensors based on the piezoelectric/triboelectric principle collect mechanical energy and their output electrical signal indicates the magnitude of force stimulus, which has been proven to be very promising to develop self-powered sensors (Zhao et al., 2019). In addition, inspired by the structural color of fish skin, a graphene coating that changed color when deformed was developed (Deng et al., 2017). The graphene coating had a periodically arranged microscopic surface structure, which caused unique interference of light, resulting in a special color-change effect regulated by strain as shown in Figure 7C. Such structural color-based strategy realizes the transformation from micromechanics to macroscopic optics and provides an outstanding visible method for mechanical sensing, which is of great significance in smart clothing worn on people, even airplanes, buildings, bridges, etc., to assess micro-crack levels and warn early dangers. Most skin electronic products are made of materials with poor air permeability. These materials limit the evaporation of sweat and cause discomfort and skin inflammation during long-term use. In order to solve the problem of air permeability, laser-induced porous graphene was used as the sensing element, and the silicone elastomer sponge with sugar as the template was used as the substrate to make a sensor which was mechanically compliant and suitable for wearing (Figure 7D) (Sun et al., 2018). More importantly, the porous structure device showed high water-vapor permeability (~18 mg cm^{-2} h^{-1}) which was 18 times higher than that of counterpart without pores, alleviating the risks of skin inflammation. In addition, the stimulus-sensitive properties of 2D materials are combined with the protective properties of functionalized textiles (such as flame retardancy, acid-alkali resistance, super mechanical properties) to fabricate intelligent protective clothing (Wang et al., 2020a), which not only retains its wearing comfort and protects human from injury but also enables the introduction of functions such as monitoring

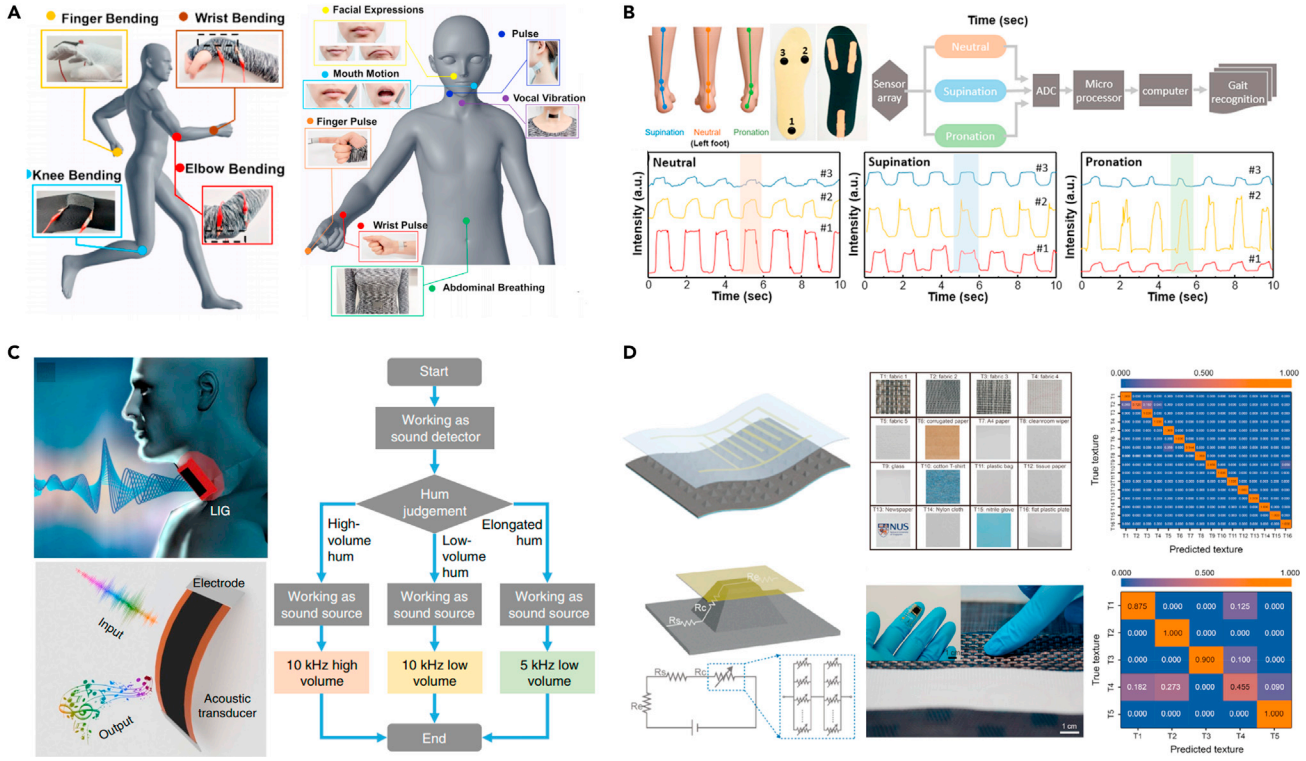

Figure 8. Wearable applications and machine learning-assisted smart sensors

(A) Graphene textile strain sensor for human motion detection;

(B) Graphene pressure sensor for various gait detection;

(C) Graphene artificial throat based on the pattern recognition and machine learning with sound-sensing and sound-emitting ability;

(D) Graphene vibrotactile sensitive sensors to recognize textures with an accuracy of 97% using a machine learning algorithm. Adapted from Refs. [(Yang et al., 2018) (Pang et al., 2018) (Tao et al., 2017), (Yao et al., 2020)].

physiological signals. The above development provides many unique functions for wearable sensors, highlighting the application potential of 2D materials in a wide range of fields.

WEARABLE APPLICATIONS

The atomic thinness of 2D materials largely miniaturizes strain or pressure sensors that will even not interfere with the surface shape and force signal distribution of the object being measured. Wearable mechanical sensors based on 2D materials withstand high strain and great bending motion, and can be applied to structures that are not suitable for metal or silicon counterparts (Akinwande et al., 2014). Thus, many challenges associated with biomedical epidermal devices and robotic manipulation would be addressed. Compared with pedometers in commercial wristbands and smart watches, wearable mechanical sensors based on 2D materials can be attached to different parts of human for detecting lots of human motion information (Boland et al., 2014; Liu et al., 2016a; Wang et al., 2014; Yang et al., 2018), such as muscle movements, pulse, respiration, facial expressions and gait (Figures 8A and 8B).

In recent years, the application of wearable mechanical sensors in the field of medical detection becomes common and has great significance for non-invasive, real-time, continuous disease monitoring, and treatment (Kim et al., 2011a, 2011b; Webb et al., 2013, 2015). For example, pulse is a very important physiological signal for evaluating the health condition of the cardiovascular system, and is usually used to distinguish the tester's age, gender, and certain diseases, such as high blood pressure. Graphene based wearable strain or pressure sensors worn on the human wrist clearly differentiated the three characteristic peaks (named percussion waves, tidal waves, and diastolic wave) in the diastolic tail of the pulse wave shape, indicating their promising potential in home-based pulse diagnosis (Yang et al., 2017a). Such wearable devices imitate the physician's tactile sensation of the pulse and provide real-time pulse waveform recording, which help bring more quantitative data analysis in the practice of traditional Chinese medicine. Wearing a flexible

mechanical sensor on a patient with a movement disorder can monitor the muscle stretching characteristics and provide a scientific basis for clinical diagnosis and treatment of neurological diseases, such as Parkinson'sdisease, muscle stiffness and stroke, as well as rehabilitation training (Lanatà et al., 2009; Wang et al., 2014). By detecting various subtle deformations of the body surface, including heartbeat, blinking, vocalization, breathing (Pang et al., 2018; Wang et al., 2014, 2015c; Yang et al., 2017a, 2018), it provides information about physical health and even inspires some new application concepts. For example, the graphene artificial throat monitored the simple throat vibrations of dumb people and converted them into controllable sounds as shown in Figure 8C (Tao et al., 2017). First, dumb people made meaningful buzzing, coughing, and screaming after passing through the training process. The artificial throat was attached on the throat of the tester and worked in detecting mode or emitting mode. In the detecting mode, the artificial throat collected the sound wave intensity or frequency corresponding to the tester, and converted it into specific meanings through pattern recognition and machine learning. In the emitting mode, the artificial throat functioned as a sound source and generated the corresponding sound signal. Such intelligent artificial throat has taken a meaningful step toward real-time barrier-free voice communication between dumb and healthy people.

As mentioned earlier, wearable mechanical sensors can identify multiple biological features related to human muscle activity which are unique and exclusive representing features of the genuine owner. Relying on the fusion of multiple biological features, such as pulse wave features and throat sound features, a self-powered bionic membrane sensor was developed to open up a new technology for multimodal biometric authentication with advantages of low-cost and simplicity in system construction (Jin et al., 2015). Although the above devices are manufactured based on nanowire structures, their application concepts are also applicable to wearable mechanical sensors using 2D materials. Wearable mechanical sensors with high performance are also applicable for robotic operations (Lim et al., 2015; Shih et al., 2020). Attaching the strain or pressure sensor to the robot's hands and feet to measure the contact force between robot and the ground or target object can help it achieve the gripping operation, normal walking or more complex motion behaviors (Sun et al., 2019). The flexible mechanical sensor also has great application potential in the field of intelligent prosthetics, which makes the prosthetic limbs completely renewed and truly replace the missing parts of the body, so that the patients have a vivid tactile experience while walking (Kim et al., 2014; Tee et al., 2015).

MACHINE LEARNING-ASSISTED SMART SENSORS

In industry and everyday life, people will increasingly make more decisions based on sensor information (Tesch da Silva et al., 2020). However, there still exists a big gap between sensor data collection and decision support systems. Rapid development of various smart structures in sensors enriched the data structural complexity, and the increasing complexity further poses a real challenge for data analysis. In special application scenario, high-dimensional or high-frequency needed to be collected from sensors for professional practice (Li et al., 2020; Su et al., 2015; Truong-Son Dinh et al., 2019). Moreover, the sensor structure design introduced in sections "Multifunction-oriented structural design" and "High performance-oriented structural design" including nonlinear data, real-time dynamic measurement and multi-axis mechanical signal further increases the level of challenge in data analysis (Ahmed et al., 2021).

One of the state-in-art analysis method to handle highly complex data structure with high accuracy is machine learning (Wang et al., 2021), which means learning from and making predictions about data by imitating the way that humans learn. By making sense of data so complex that defies human analysis, algorithms based on machine learning technology could improve its classification and prediction accuracy. Technically, machine learning algorithm utilizes a mathematic model that general enough to fit the highly nonlinear relations between input and output data (LeCun et al., 2015). The most popular algorithm, deep neural network (DNN) model (Ioffe and Szegedy, 2015), utilized a network with multiple layers to construct a highly nonlinear structure. One of the most successful application scenario of DNN is computer vision (Dawar and Kehtarnavaz, 2018): the complexity relations between images (or videos) and objects (or event) can be accurately modeled by convolutional neural network (CNN), which is a special type of DNN. Another popular algorithm is decision trees, which takes advantage of nonlinearity from tree-structure. The classic algorithm, support vector machine (SVM) (Burges, 1998), utilize kernels to implement nonlinearity in classification and is proved to be highly efficiency in medium sized data.

According to the characteristic of sensing data structure, eligible mathematical model would be selected. Common mathematical models include cluster analysis, CNN, decision trees, and SVM. The machine learning architecture could also combine with specific data pretreatment in special application scene. For high-frequency data analysis, learning architecture could integrate time-frequency analysis algorithms (Xiong et al., 2021), such as wavelet analysis, and short-time Fourier transform. For high-dimensional data analysis, learning architecture could integrate dimensionality reduction algorithm (Anzenbacher et al., 2012), such as principal component analysis (PCA), factor analysis, and autoencoder. Efficient and accurate data analysis method based on machine learning are interfacing with sensor information collection and decision support systems.

Therefore, combining wearable sensors with machine learning and artificial intelligence technologies to build machine learning-assisted smart sensors will provide unique opportunities for emerging smart wearable electronic products. Smart sensors usually include basic sensitive units and artificial intelligence modules. The sensitive units respond quickly and accurately to the detected target. The artificial intelligence modules assist sensing feature extraction and pattern recognition through the machine learning algorithm, and finally transmit the recognized pattern state to the user through an easy-to-operate platform. The above-mentioned smart sensors can not only collect but also analyze the sensing data, especially for some application scenarios that need to judge the perception content in a timely manner to accurately process complex operation tasks (Shih et al., 2020; Zhou et al., 2020). These operational tasks include but are not limited to: determining the treatment plan based on the diagnosis mode reflected by the collected data, artificial prostheses that help people with walk disabilities and intelligent robots that respond to complex operations in high-risk environments. Up to now, machine learning-assisted smart sensors have been applied in both industrial sector and everyday life. Industrial applications include aerodynamic parameter detection (Xiong et al., 2021), mechanical faults diagnostic (Rabelo Baccarini et al., 2011), food-freshness prediction (Guo et al., 2020), industrial soft sensing (Shao et al., 2020), etc. For every-day life, smart sensors are widely applied in physiological processes and sleep patterns detection (Lee et al., 2020), human gesture recognition (HGR) (Wang et al., 2020b; Zhou et al., 2020), *etc.*

For example, by uniformly coating graphene on a microstructured elastomer, environment-resilient graphene based vibrotactile sensitive sensors were developed, demonstrating the sensing ability to recognize specific patterns and textures with the help of machine learning algorithms as shown in Figure 8D (Yao et al., 2020). The sensor reliably responded to pressure changes under different environmental conditions (25–60°C and 30–90% relative humidity), with performance changes less than 5% and 3% respectively, and it also responded to vibration signals up to 1500 Hz with good response. Due to the fast and reliable vibration response of the sensors, the sensors accurately reflected the characteristic frequency compositions of 16 common textures that interact with people. After the k-nearest neighbors machine learning algorithm was used to classify and recognize texture frequency compositions, the recognition results show up to 97% accuracy. This machine learning-assisted texture recognition method has potential in the application scenarios of robots and artificial prosthetic skins. In addition, the fusion of multi-stimulus sensing modes (force stimulation, other physical, chemical or biological stimuli) with the help of machine learning algorithms will meet more functional scene sensing requirements. For example, a graphene-based sensor prepared by laser engraving reduction simultaneously monitored temperature, breathing rate, and sweat composition (Yang et al., 2019b). This on-skin type sensor collected data from healthy people and patients. After training through machine learning algorithms, it could analyze the differences in various physiological parameters of the volunteers, and then provided a basis for the diagnosis of related diseases, such as gout and metabolic disorders.

FUTURE PERSPECTIVES

This review summarizes the latest development of 2D materials based flexible and stretchable mechanical sensors from the perspectives of sensing mechanism, material structure designs and wearable applications. These sensors demonstrate their wide-ranging applications in daily health, sports science, human-computer interaction, and so on. Although a lot of progress has been made in the past few decades, most of 2D materials-based sensors are still in the prototype stage and their appeal to consumers is still limited. Challenges and future development opportunities involve efforts to develop multifunctional sensors that are comfortable to wear.

First, due to the curved structure of the human body, how the 2D materials based mechanical sensors can better fit the human body and meet the needs of wearing comfort is the key content that needs more exploration in the future. The skin usually undergoes a series of complex deformations at different body positions. Mechanical sensors need to provide compliance and location-specific measurement ranges through innovative structural engineering designs (Kim et al., 2014). The fusion of 2D materials with other flexible functional materials, especially smart fabrics, will be an important way to achieve wearable comfort. In addition, wearability requires the sensor to have high performance, small size, light weight, low power consumption, and robustness to reduce the requirements for the related signal acquisition and chip processing system, so that the entire sensor system has a long standby and lifetime under the premise of minimizing the system size.

Second, with the continuous enrichment of people's daily life applications, the functional requirements for sensors to sense physical signals are increasing. Having multiple functions and showing unique responses to external stimuli is still the development trend of 2D materials-based mechanical sensor technology. It seems to be realistic in future to combine multi-functional wearable sensors with skin and clothes. The goal is to be able to cover complex-shaped surfaces and moving parts to form artificial electronic skin or smart clothing, which is oriented to artificial touch and flexible medical care. Most of the current work is still stuck in single-function sensor devices, lacking conceptual multi-function and system integrated design. In fact, human touch is based on comprehensive activities of sensing, refining, and learning. The receptors in the skin detect touch, and the signal is sent to neurons through the axis to obtain the multilevel characteristics of the touch. Therefore, wearable mechanical sensors with this perceptual learning ability may expand their cognitive capabilities and adaptability. To achieve this goal, multifunction-oriented system-level structural design will be an essential and useful tool. For example, an artificial sensory neuron with the capability of tactile perceptual learning has been developed, including a resistive pressure sensor that senses, a soft ionic cable that transmits, and a synaptic transistor that processes information (Changjin et al., 2018). This device could recognize the spatiotemporal features of touched patterns. After the machine learning training process, the recognition error rate was greatly reduced from 44% to 0.4%. Combining wearable sensor technology with artificial intelligence technology, and in-depth study of the characteristics of the massive data collected by sensors, will bring innovative and interesting applications, which are still in their infancy.

Thirdly, the integration of devices and 2D materials is still a very challenging task, resulting in sensors based on 2D materials still far from real life. First of all, it is necessary to realize the large-area integration of nano features/micro-nano structures/macro devices on flexible substrates of arbitrary shapes. The precise formation of functional interfaces involving materials with very different electromechanical properties (such as polymers, 2D layers, and other functional layers) poses a great challenge to its manufacturing technology. It is necessary to develop device designs and manufacturing processes that match the electromechanical characteristics of 2D layers, and strengthen the adhesion between the 2D layer and the substrate, so that the device is stable and durable. Moreover, to realize such a highly integrated smart sensor system based on 2D materials requires the integration of different flexible functional devices, such as the combination of sensors and thin film transistors to manufacture mechanical sensing active matrix. Capacitive sensors are usually used as the gate dielectric of the transistor, and resistive sensors are usually connected to the drain of the transistor. However, although 2D materials have proven to be promising for the fabrication of electrode and channel materials in transistor-type device (Zheng et al., 2021a), it is still difficult to synthesize 2D layers and their heterojunctions with controlled defects and number of layers at the wafer level. In addition, the existing synthesis technology often has disadvantages such as high cost, complicated process, incompatibility with organic materials, and lack of research on stretchability. Another challenge is how to enhance the performance consistency of sensor units manufactured in different batches, which is very important for large-area integrated manufacturing to reduce unnecessary complex calibration. The mechanic-sensitive structure of 2D materials is very rich, including geometric elements such as fracture, buckling, and pores, and so on. The manufacturing of this type of structure is currently random and uncontrollable. It is necessary to strengthen the understanding of the physical and chemical behavior of the 2D interface, and to study solution-compatible processes (such as the printing processes (Conti et al., 2020; Li et al., 2014)) to realize the large-area fine and controllable batch preparation of micro-nano mechanic-sensitive structures and integrated electronics, which is the key to moving from the laboratory to industrial applications.

ACKNOWLEDGMENTS

This work was supported by the National Natural Science Foundation of China (51802293, 52172046), the Basic Science Center Project of NSFC (51788104) and the Fundamental Research Funds for the Central Universities (2682021CX120).

AUTHOR CONTRIBUTIONS

Conceptualization, T.T.Y. and H.W.Z.; Investigation, T.T.Y., Y.H.H. and L.Z.; Writing (Original Draft), T.T.Y. and X.J.; Writing (Review& Editing), T.T.Y., Q.T., Z.H.D. and H.W.Z.; Supervision, H.W.Z.; Funding Acquisition, T.T.Y and H.W.Z.

DECLARATION OF INTERESTS

The authors declare no competing interests.

REFERENCES

Addou, R., Colombo, L., and Wallace, R.M. (2015). Surface defects on natural MoS_2. ACS Appl. Mater. Inter. *7*, 11921–11929.

Ahmed, M.A., Zaidan, B.B., Zaidan, A.A., Salih, M.M., Al-qaysi, Z.T., and Alamoodi, A.H. (2021). Based on wearable sensory device in 3D-printed humanoid: a new real-time sign language recognition system. Measurement *168*, 108431.

Akinwande, D., Petrone, N., and Hone, J. (2014). Two-dimensional flexible nanoelectronics. Nat. Commun. *5*, 5678.

Akinwande, D., Brennan, C.J., Bunch, J.S., Egberts, P., Felts, J.R., Gao, H., Huang, R., Kim, J.-S., Li, T., and Li, Y. (2017). A review on mechanics and mechanical properties of 2D materials—graphene and beyond. Extreme Mech. Lett. *13*, 42–77.

Androulidakis, C., Zhang, K., Robertson, M., and Tawfick, S. (2018). Tailoring the mechanical properties of 2D materials and heterostructures. 2d Mater. *5*, 032005.

Anzenbacher, P., Li, F., and Palacios, M.A. (2012). Toward wearable sensors: fluorescent attoreactor mats as optically encoded cross-reactive sensor arrays. Angew.Chem. Int. Ed. *51*, 2345–2348.

Bae, S.-H., Lee, Y., Sharma, B.K., Lee, H.-J., Kim, J.-H., and Ahn, J.-H. (2013). Graphene-based transparent strain sensor. Carbon *51*, 236–242.

Banhart, F., Kotakoski, J., and Krasheninnikov, A.V. (2010). Structural defects in graphene. ACS Nano *5*, 26–41.

Boland, C.S., Khan, U., Backes, C., O'Neill, A., McCauley, J., Duane, S., Shanker, R., Liu, Y., Jurewicz, I., and Dalton, A.B. (2014). Sensitive, high-strain, high-rate bodily motion sensors based on graphene–rubber composites. ACS Nano *8*, 8819–8830.

Boland, C.S., Khan, U., Ryan, G., Barwich, S., Charifou, R., Harvey, A., Backes, C., Li, Z., Ferreira, M.S., and Möbius, M.E. (2016). Sensitive electromechanical sensors using viscoelastic graphene-polymer nanocomposites. Science *354*, 1257–1260.

Brennan, C.J., Nguyen, J., Yu, E.T., and Lu, N. (2015). Interface adhesion between 2D materials and elastomers measured by buckle delaminations. Adv. Mater. Inter. *2*, 1500176.

Bückmann, T., Stenger, N., Kadic, M., Kaschke, J., Frölich, A., Kennerknecht, T., Eberl, C., Thiel, M., and Wegener, M. (2012). Tailored 3D mechanical metamaterials made by dip-in direct-laser-writing optical lithography. Adv. Mater. *24*, 2710–2714.

Burges, C.J.C. (1998). A tutorial on support vector machines for pattern recognition. Data Min. Knowl. Disc. *2*, 121–167.

Cai, Y.-W., Zhang, X.-N., Wang, G.-G., Li, G.-Z., Zhao, D.-Q., Sun, N., Li, F., Zhang, H.-Y., Han, J.-C., and Yang, Y. (2021). A flexible ultra-sensitive triboelectric tactile sensor of wrinkled PDMS/MXene composite films for E-skin. Nano Energy *81*, 105663.

Chang, C.-H., Fan, X., Lin, S.-H., and Kuo, J.-L. (2013). Orbital analysis of electronic structure and phonon dispersion in MoS_2, $MoSe_2$, WS_2, and WSe_2 monolayers under strain. Phys. Rev. B *88*, 195420.

Chang, Y., Wang, L., Li, R., Zhang, Z., Wang, Q., Yang, J., Guo, C.F., and Pan, T. (2021). First decade of interfacial iontronic sensing: from droplet sensors to artificial skins. Adv. Mater. *33*, 2003464.

Changjin, W., Geng, C., Yangming, F., Ming, W., Naoji, M., Shaowu, P., Liang, P., Hui, Y., Qing, W., and Liqiang, Z. (2018). An artificial sensory neuron with tactile perceptual learning. Adv. Mater. *30*, 1801291.

Chao, M., He, L., Gong, M., Li, N., Li, X., Peng, L., Shi, F., Zhang, L., and Wan, P. (2021). Breathable Ti_3C_2Tx MXene/protein nanocomposites for ultrasensitive medical pressure sensor with degradability in solvents. ACS Nano *15*, 9746–9758.

Chen, C. (2013). Graphene Nanoelectromechanical Resonators and Oscillators (Columbia University).

Chen, Z., Ren, W., Gao, L., Liu, B., Pei, S., and Cheng, H.-M. (2011). Three-dimensional flexible and conductive interconnected graphene networks grown by chemical vapour deposition. Nat. Mater. *10*, 424.

Chen, Y.-M., He, S.-M., Huang, C.-H., Huang, C.-C., Shih, W.-P., Chu, C.-L., Kong, J., Li, J., and Su, C.-Y. (2016a). Ultra-large suspended graphene as a highly elastic membrane for capacitive pressure sensors. Nanoscale *8*, 3555–3564.

Chen, Z., Ming, T., Goulamaly, M.M., Yao, H., Nezich, D., Hempel, M., Hofmann, M., and Kong, J. (2016b). Enhancing the sensitivity of percolative graphene films for flexible and transparent pressure sensor arrays. Adv. Funct. Mater. *26*, 5061–5067.

Chen, D., Wang, D., Yang, Y., Huang, Q., Zhu, S., and Zheng, Z. (2017a). Self-healing materials for next-generation energy harvesting and storage devices. Adv. Energy Mater. *7*, 1700890.

Chen, X., Han, X., and Shen, Q.D. (2017b). PVDF-based ferroelectric polymers in modern flexible electronics. Adv. Electron. Mater. *3*, 1600460.

Chen, Z., Wang, Z., Li, X., Lin, Y., Luo, N., Long, M., Zhao, N., and Xu, J.-B. (2017c). Flexible piezoelectric-induced pressure sensors for static measurements based on nanowires/graphene heterostructures. ACS Nano *11*, 4507–4513.

Chen, M., Wang, Z., Ge, X., Wang, Z., Fujisawa, K., Xia, J., Zeng, Q., Li, K., Zhang, T., and Zhang, Q. (2019). Controlled fragmentation of single-atom-thick polycrystalline graphene. Matter *2*, 666–679.

Cheng, Y., Wang, R., Sun, J., and Gao, L. (2015). A stretchable and highly sensitive graphene-based fiber for sensing tensile strain, bending, and torsion. Adv. Mater. *27*, 7365–7371.

Cheng, L., Zhang, C., and Liu, Y. (2019). The optimal electronic structure for high-mobility 2d semiconductors: exceptionally high hole mobility in 2d antimony. J. Am. Chem. Soc. *141*, 16296–16302.

Choi, J.S., Kim, J.-S., Byun, I.-S., Lee, D.H., Lee, M.J., Park, B.H., Lee, C., Yoon, D., Cheong, H., and Lee, K.H. (2011). Friction anisotropy–driven domain imaging on exfoliated monolayer graphene. Science *333*, 607–610.

Choi, W., Kim, J., Lee, E., Mehta, G., and Prasad, V. (2021). Asymmetric 2D MoS_2 for scalable and high-performance piezoelectric sensors. ACS Appl. Mater. Inter. *13*, 13596–13603.

Chu, H., Jang, H., Lee, Y., Chae, Y., and Ahn, J.-H. (2016). Conformal, graphene-based triboelectric nanogenerator for self-powered wearable electronics. Nano Energy *27*, 298–305.

Cocco, G., Cadelano, E., and Colombo, L. (2010). Gap opening in graphene by shear strain. Phys. Rev. B *81*, 241412.

Conti, S., Pimpolari, L., Calabrese, G., Worsley, R., Majee, S., Polyushkin, D.K., Paur, M., Pace, S., Keum, D.H., and Fabbri, F. (2020). Low-voltage 2D materials-based printed field-effect transistors for integrated digital and analog electronics on paper. Nat. Commun. *11*, 1–9.

Cui, C., Xue, F., Hu, W.-J., and Li, L.-J. (2018). Two-dimensional materials with piezoelectric and ferroelectric functionalities. Npj 2d Mater. Appl. *2*, 1–14.

D'Elia, E., Barg, S., Ni, N., Rocha, V.G., and Saiz, E. (2015). Self-healing graphene-based composites with sensing capabilities. Adv. Mater. *27*, 4788–4794.

Dai, Z., Hou, Y., Sanchez, D.A., Wang, G., Brennan, C.J., Zhang, Z., Liu, L., and Lu, N. (2018). Interface-governed deformation of nanobubbles and nanotents formed by two-dimensional materials. Phys. Rev. Lett. *121*, 266101.

Dai, M., Wang, Z., Wang, F., Qiu, Y., Zhang, J., Xu, C.-Y., Zhai, T., Cao, W., Fu, Y., and Jia, D. (2019a). Two-Dimensional van der Waals Materials with aligned in-plane polarization and large piezoelectric effect for self-powered piezoelectric sensors. Nano Lett. *19*, 5410–5416.

Dai, Z., Liu, L., and Zhang, Z. (2019b). Strain engineering of 2D materials: issues and opportunities at the interface. Adv. Mater. *31*, 1805417.

Davidovikj, D., Scheepers, P.H., van der Zant, H.S., and Steeneken, P.G. (2017). Static capacitive pressure sensing using a single graphene drum. ACS Appl. Mater. Inter. *9*, 43205–43210.

Dawar, N., and Kehtarnavaz, N. (2018). Action detection and recognition in continuous action streams by deep learning-based sensing fusion. IEEE Sens. J. *18*, 9660–9668.

Deng, S., and Berry, V. (2016). Wrinkled, rippled and crumpled graphene: an overview of formation mechanism, electronic properties, and applications. Mater. Today *19*, 197–212.

Deng, Y., Gao, S., Liu, J., Gohs, U., Mäder, E., and Heinrich, G. (2017). Variable structural colouration of composite interphases. Mater.Horiz. *4*, 389–395.

Deng, C., Gao, P., Lan, L., He, P., and Cao, Y. (2019). Ultrasensitive and highly stretchable multifunctional strain sensors with timbre-recognition ability based on vertical graphene. Adv. Funct. Mater. *29*, 1907151.

Deng, C., Lan, L., He, P., Ding, C., Chen, B., Zheng, W., Zhao, X., Chen, W., Zhong, X., and Li, M. (2020). High-performance capacitive strain sensors with highly stretchable vertical graphene electrodes. J. Mater. Chem. C *8*, 5541–5546.

Van Der Zande, A.M., Huang, P.Y., Chenet, D.A., Berkelbach, T.C., You, Y., Lee, G.-H., Heinz, T.F., Reichman, D.R., Muller, D.A., and Hone, J.C. (2013). Grains and grain boundaries in highly crystalline monolayer molybdenum disulphide. Nat. Mater. *12*, 554.

Dinh Le, T.-S., An, J., Huang, Y., Vo, Q., Boonruangkan, J., Tran, T., Kim, S.-W., Sun, G., and Kim, Y.-J. (2019). Ultrasensitive anti-interference voice recognition by bio-inspired skin-attachable self-cleaning acoustic sensors. ACS Nano *13*, 13293–13303.

Duerloo, K.-A.N., Ong, M.T., and Reed, E.J. (2012). Intrinsic piezoelectricity in two-dimensional materials. J. Phys. Chem. Lett. *3*, 2871–2876.

Eswaraiah, V., Balasubramaniam, K., and Ramaprabhu, S. (2011). Functionalized graphene reinforced thermoplastic nanocomposites as strain sensors in structural health monitoring. J. Mater. Chem. *21*, 12626–12628.

Falin, A., Cai, Q., Santos, E.J., Scullion, D., Qian, D., Zhang, R., Yang, Z., Huang, S., Watanabe, K., and Taniguchi, T. (2017). Mechanical properties of atomically thin boron nitride and the role of interlayer interactions. Nat.Commun *8*, 15815.

Fan, X., Forsberg, F., Smith, A.D., Schröder, S., Wagner, S., Rödjegård, H., Fischer, A.C., Östling, M., Lemme, M.C., and Niklaus, F. (2019). Graphene ribbons with suspended masses as transducers in ultra-small nanoelectromechanical accelerometers. Nat. Electron. *2*, 394–404.

Fei, R., Li, W., Li, J., and Yang, L. (2015). Giant piezoelectricity of monolayer group IV monochalcogenides: SnSe, SnS, GeSe, and GeS. Appl. Phys. Lett. *107*, 173104.

Fei, R., Kang, W., and Yang, L. (2016). Ferroelectricity and phase transitions in monolayer group-IV monochalcogenides. Phys. Rev. Lett. *117*, 097601.

Fratzl, P., and Barth, F.G. (2009). Biomaterial systems for mechanosensing and actuation. Nature *462*, 442–448.

Fu, X.-W., Liao, Z.-M., Zhou, J.-X., Zhou, Y.-B., Wu, H.-C., Zhang, R., Jing, G., Xu, J., Wu, X., and Guo, W. (2011). Strain dependent resistance in chemical vapor deposition grown graphene. Appl. Phys. Lett. *99*, 213107.

Gao, Y., Kim, S., Zhou, S., Chiu, H.-C., Nélias, D., Berger, C., De Heer, W., Polloni, L., Sordan, R., and Bongiorno, A. (2015). Elastic coupling between layers in two-dimensional materials. Nat. Mater. *14*, 714.

Gao, L., Wang, M., Wang, W., Xu, H., Wang, Y., Zhao, H., Cao, K., Xu, D., and Li, L. (2021). Highly sensitive pseudocapacitive iontronic pressure sensor with broad sensing range. Nano-micro Lett. *13*, 1–14.

Garcia, C., Trendafilova, I., de Villoria, R.G., and del Rio, J.S. (2018). Self-powered pressure sensor based on the triboelectric effect and its analysis using dynamic mechanical analysis. Nano Energy *50*, 401–409.

Geim, A.K., and Grigorieva, I.V. (2013). Van der Waals heterostructures. Nature *499*, 419–425.

Gong, L., Kinloch, I.A., Young, R.J., Riaz, I., Jalil, R., and Novoselov, K.S. (2010). Interfacial stress transfer in a graphene monolayer nanocomposite. Adv. Mater. *22*, 2694–2697.

Gui, G., Li, J., and Zhong, J. (2008). Band structure engineering of graphene by strain: first-principles calculations. Phys. Rev. B *78*, 075435.

Guo, H., Yeh, M.-H., Lai, Y.-C., Zi, Y., Wu, C., Wen, Z., Hu, C., and Wang, Z.L. (2016). All-in-one shape-adaptive self-charging power package for wearable electronics. ACS Nano *10*, 10580–10588.

Guo, L., Wang, T., Wu, Z., Wang, J., Wang, M., Cui, Z., Ji, S., Cai, J., Xu, C., and Chen, X. (2020). Portable food-freshness prediction platform based on colorimetric barcode combinatorics and deep convolutional neural networks. Adv. Mater. *32*, 2004805.

Han, E., Yu, J., Annevelink, E., Son, J., Kang, D.A., Watanabe, K., Taniguchi, T., Ertekin, E., Huang, P.Y., and van der Zande, A.M. (2020). Ultrasoft slip-mediated bending in few-layer graphene. Nat. Mater. *19*, 305–309.

He, X., Liu, Z., Shen, G., He, X., Liang, J., Zhong, Y., Liang, T., He, J., Xin, Y., and Zhang, C. (2021). Microstructured capacitive sensor with broad detection range and long-term stability for human activity detection. Npj Flex. Electron. *5*, 1–9.

Hempel, M., Nezich, D., Kong, J., and Hofmann, M. (2012). A novel class of strain gauges based on layered percolative films of 2D materials. Nano Lett. *12*, 5714–5718.

Hosseini, M., Elahi, M., Pourfath, M., and Esseni, D. (2015a). Strain-induced modulation of electron mobility in single-layer transition metal dichalcogenides MX_2 (M=Mo,W; X=S, Se). IEEE T. Electron Dev. *62*, 3192–3198.

Hosseini, M., Elahi, M., Pourfath, M., and Esseni, D. (2015b). Very large strain gauges based on single layer MoSe2 and WSe2 for sensing applications. Appl. Phys. Lett. *107*, 253503.

Hou, C., Wang, H., Zhang, Q., Li, Y., and Zhu, M. (2014). Highly conductive, flexible, and compressible all-graphene passive electronic skin for sensing human touch. Adv. Mater. *26*, 5018–5024.

Hu, T., and Dong, J. (2016). Two new phases of monolayer group-IV monochalcogenides and their piezoelectric properties. Phys. Chem. Chem. Phys. *18*, 32514–32520.

Huang, M., Pascal, T.A., Kim, H., Goddard, W.A., III, and Greer, J.R. (2011). Electronic– mechanical coupling in graphene from in situ nanoindentation experiments and multiscale atomistic simulations. Nano Lett. *11*, 1241–1246.

Huang, H., Su, S., Wu, N., Wan, H., Wan, S., Bi, H., and Sun, L. (2019a). Graphene-based sensors for human health monitoring. Front. Chem. *7*, 399.

Huang, T., He, P., Wang, R., Yang, S., Sun, J., Xie, X., and Ding, G. (2019b). Porous fibers composed of polymer nanoball decorated graphene for wearable and highly sensitive strain sensors. Adv. Funct. Mater. *29*, 1903732.

Ioffe, S., and Szegedy, C. (2015). Batch normalization: accelerating deep network training by reducing internal covariate shift. In International Conference on Machine Learning, *37* (Proceedings of Machine Learning Research), pp. 448–456.

Jian, M., Xia, K., Wang, Q., Yin, Z., Wang, H., Wang, C., Xie, H., Zhang, M., and Zhang, Y. (2017). Flexible and highly sensitive pressure sensors based on bionic hierarchical structures. Adv. Funct. Mater. *27*, 1606066.

Jiang, T., Huang, R., and Zhu, Y. (2014). Interfacial sliding and buckling of monolayer graphene on a stretchable substrate. Adv. Funct. Mater. *24*, 396–402.

Jiang, H., Zheng, L., Liu, Z., and Wang, X. (2020). Two-dimensional materials: from mechanical properties to flexible mechanical sensors. InfoMat *2*, 1077–1094.

Jin, Y., Chen, J., Su, Y., Jing, Q., and Zhong, L.W. (2015). Eardrum-inspired active sensors for self-powered cardiovascular system characterization and throat-attached anti-interference voice recognition. Adv. Mater. *27*, 1316–1326.

Jing, Z., Guang-Yu, Z., and Dong-Xia, S. (2013). Review of graphene-based strain sensors. Chin. Phys. B *22*, 057701.

Jones, J., Lacour, S.P., Wagner, S., and Suo, Z. (2004). Stretchable wavy metal interconnects. J. Vacuum Sci. Technol. A Vacuum, Surf. Films *22*, 1723–1725.

Jung, Y.H., Park, B., Kim, J.U., and Kim, T. (2019). Bioinspired electronics: bioinspired electronics for artificial sensory systems. Adv. Mater. *31*, 1970242.

Kang, D., Pikhitsa, P.V., Choi, Y.W., Lee, C., Shin, S.S., Piao, L., Park, B., Suh, K.-Y., Kim, T.-i., and Choi, M. (2014). Ultrasensitive mechanical crack-based sensor inspired by the spider sensory system. Nature *516*, 222–226.

Kang, S., Lee, J., Lee, S., Kim, S., Kim, J.K., Algadi, H., Al-Sayari, S., Kim, D.E., Kim, D., and Lee, T. (2016). Highly sensitive pressure sensor based on bioinspired porous structure for real-time tactile sensing. Adv. Electron. Mater. *2*, 1600356.

Kang, M., Kim, J., Jang, B., Chae, Y., Kim, J.-H., and Ahn, J.-H. (2017). Graphene-based three-dimensional capacitive touch sensor for wearable electronics. ACS Nano *11*, 7950–7957.

Kim, D.-H., Lu, N., Ghaffari, R., Kim, Y.-S., Lee, S.P., Xu, L., Wu, J., Kim, R.-H., Song, J., and Liu, Z. (2011a). Materials for multifunctional balloon catheters with capabilities in cardiac electrophysiological mapping and ablation therapy. Nat. Mater. *10*, 316.

Kim, D.-H., Lu, N., Ma, R., Kim, Y.-S., Kim, R.-H., Wang, S., Wu, J., Won, S.M., Tao, H., and Islam, A. (2011b). Epidermal electronics. Science *333*, 838–843.

Kim, Y.-J., Cha, J.Y., Ham, H., Huh, H., So, D.-S., and Kang, I. (2011c). Preparation of piezoresistive nano smart hybrid material based on graphene. Curr.Appl. Phys. *11*, S350–S352.

Kim, J., Lee, M., Shim, H.J., Ghaffari, R., Cho, H.R., Son, D., Jung, Y.H., Soh, M., Choi, C., and Jung, S. (2014). Stretchable silicon nanoribbon electronics for skin prosthesis. Nat. Commun. *5*, 5747.

Kim, J., Lee, E., Bhoyate, S., and An, T.K. (2020). Stable and high-performance piezoelectric sensor via CVD grown WS2. Nanotechnology *31*, 445203.

Koyama, M., Zhang, Z., Wang, M., Ponge, D., Raabe, D., Tsuzaki, K., Noguchi, H., and Tasan, C.C. (2017). Bone-like crack resistance in hierarchical metastable nanolaminate steels. Science *355*, 1055–1057.

Kumar, H., Dong, L., and Shenoy, V.B. (2016). Limits of coherency and strain transfer in flexible 2D van der waals heterostructures: formation of strain solitons and interlayer debonding. Sci. Rep. *6*, 21516.

Lan, L., Yin, T., Jiang, C., Li, X., Yao, Y., Wang, Z., Qu, S., Ye, Z., Ping, J., and Ying, Y. (2019). Highly conductive 1D-2D composite film for skin-mountable strain sensor and stretchable triboelectric nanogenerator. Nano Energy *62*, 319–328.

Lan, L., Zhao, F., Yao, Y., Ping, J., and Ying, Y. (2020). One-step and spontaneous in situ growth of popcorn-like nanostructures on stretchable double-twisted fiber for ultrasensitive textile pressure sensor. ACS Appl. Mater. Inter. *12*, 10689–10696.

Lanatà, A., Scilingo, E.P., Nardini, E., Loriga, G., Paradiso, R., and De-Rossi, D. (2009). Comparative evaluation of susceptibility to motion artifact in different wearable systems for monitoring respiratory rate. IEEE T. Inf. Technol. B. *14*, 378–386.

Lanza, M., Wang, Y., Bayerl, A., Gao, T., Porti, M., Nafria, M., Liang, H., Jing, G., Liu, Z., and Zhang, Y. (2013). Tuning graphene morphology by substrate towards wrinkle-free devices: experiment and simulation. J. Appl. Phys. *113*, 104301.

LeCun, Y., Bengio, Y., and Hinton, G. (2015). Deep learning. Nature *521*, 436–444.

Lee, C., Wei, X., Kysar, J.W., and Hone, J. (2008). Measurement of the elastic properties and intrinsic strength of monolayer graphene. Science *321*, 385–388.

Lee, J.H., Singer, J.P., and Thomas, E.L. (2012). Micro-/nanostructured mechanical metamaterials. Adv. Mater. *24*, 4782–4810.

Lee, S.-M., Kim, J.-H., and Ahn, J.-H. (2015). Graphene as a flexible electronic material: mechanical limitations by defect formation and efforts to overcome. Mater. Today *18*, 336–344.

Lee, K., Ni, X., Lee, J.Y., Arafa, H., Pe, D.J., Xu, S., Avila, R., Irie, M., Lee, J.H., Easterlin, R.L., et al. (2020). Mechano-acoustic sensing of physiological processes and body motions via a soft wireless device placed at the suprasternal notch. Nat. Biomed. Eng. *4*, 148–158.

Li, X., Sun, P., Fan, L., Zhu, M., Wang, K., Zhong, M., Wei, J., Wu, D., Cheng, Y., and Zhu, H. (2012a). Multifunctional graphene woven fabrics. Sci. Rep. *2*, 395.

Li, X., Zhang, R., Yu, W., Wang, K., Wei, J., Wu, D., Cao, A., Li, Z., Cheng, Y., and Zheng, Q. (2012b). Stretchable and highly sensitive graphene-on-polymer strain sensors. Sci. Rep. *2*, 870.

Li, J., Lemme, M.C., and Östling, M. (2014). Inkjet printing of 2D layered materials. Chem. Phys. Chem. *15*, 3427–3434.

Li, M.-Y., Chen, C.-H., Shi, Y., and Li, L.-J. (2016a). Heterostructures based on two-dimensional layered materials and their potential applications. Mater. Today *19*, 322–335.

Li, X., Yang, T., Yang, Y., Zhu, J., Li, L., Alam, F.E., Li, X., Wang, K., Cheng, H., and Lin, C.T. (2016b). Large-area ultrathin graphene films by single-step marangoni self-assembly for highly sensitive strain sensing application. Adv. Funct. Mater. *26*, 1322–1329.

Li, Y., Zheng, C., Liu, S., Huang, L., Fang, T., Li, J.X., Xu, F., and Li, F. (2020). Smart glove integrated with tunable MWNTs/PDMS fibers made of a one-step extrusion method for finger dexterity, gesture, and temperature recognition. ACS Appl. Mater. Inter. *12*, 23764–23773.

Liechti, K. (2019). Characterizing the interfacial behavior of 2D materials: a review. Exp. Mech. *59*, 395–412.

Lim, S., Son, D., Kim, J., Lee, B.B., Song, J.K., Choi, S., Lee, D.J., Kim, J.H., Lee, M., Hyeon, T., and Kim, D.H. (2015). Transparent and stretchable interactive human machine interface based on patterned graphene heterostructures. Adv. Funct. Mater. *25*, 375–383.

Lin, S., Zhao, X., Jiang, X., Wu, A., Ding, H., Zhong, Y., Li, J., Pan, J., Liu, B., and Zhu, H. (2019). Highly stretchable, adaptable, and durable strain sensing based on a bioinspired dynamically cross-linked graphene/polymer composite. Small *15*, 1900848.

Liu, Z., Qi, D., Guo, P., Liu, Y., Zhu, B., Yang, H., Liu, Y., Li, B., Zhang, C., and Yu, J. (2015). Thickness-gradient films for high gauge factor stretchable strain sensors. Adv. Mater. *27*, 6230–6237.

Liu, Q., Chen, J., Li, Y., and Shi, G. (2016a). High-performance strain sensors with fish-scale-like graphene-sensing layers for full-range detection of human motions. ACS Nano *10*, 7901–7906.

Liu, W., Chen, Z., Zhou, G., Sun, Y., Lee, H.R., Liu, C., Yao, H., Bao, Z., and Cui, Y. (2016b). 3D porous sponge-inspired electrode for stretchable lithium-ion batteries. Adv. Mater. *28*, 3578–3583.

Liu, Y., Weiss, N.O., Duan, X., Cheng, H.-C., Huang, Y., and Duan, X. (2016c). Van der Waals heterostructures and devices. Nat. Rev. Mater. *1*, 16042.

Liu, H., Dong, M., Huang, W., Gao, J., Dai, K., Guo, J., Zheng, G., Liu, C., Shen, C., and Guo, Z. (2017a). Lightweight conductive graphene/thermoplastic polyurethane foams with ultrahigh compressibility for piezoresistive sensing. J. Mater. Chem. C *5*, 73–83.

Liu, Y., He, K., Chen, G., Leow, W.R., and Chen, X. (2017b). Nature-inspired structural materials for flexible electronic devices. Chem. Rev. *117*, 12893–12941.

Liu, H., Chen, X., Zheng, Y., Zhang, D., Zhao, Y., Wang, C., Pan, C., Liu, C., and Shen, C. (2021). Lightweight, superelastic, and hydrophobic polyimide nanofiber/MXene composite aerogel for wearable piezoresistive sensor and oil/water

separation applications. Adv. Funct. Mater. *31*, 2008006.

Lloyd, D., Liu, X., Christopher, J.W., Cantley, L., Wadehra, A., Kim, B.L., Goldberg, B.B., Swan, A.K., and Bunch, J.S. (2016). Band gap engineering with ultralarge biaxial strains in suspended monolayer MoS_2. Nano Lett. *16*, 5836–5841.

Lou, Z., Chen, S., Wang, L., Jiang, K., and Shen, G. (2016). An ultra-sensitive and rapid response speed graphene pressure sensors for electronic skin and health monitoring. Nano Energy *23*, 7–14.

Lu, Y., Biswas, M.C., Guo, Z., Jeon, J.-W., and Wujcik, E.K. (2019). Recent developments in bio-monitoring via advanced polymer nanocomposite-based wearable strain sensors. Biosens.Bioelectron. *123*, 167–177.

Mahapatra, S.D., Mohapatra, P.C., Aria, A.I., Christie, G., Mishra, Y.K., Hofmann, S., and Thakur, V.K. (2021). Piezoelectric materials for energy harvesting and sensing applications: roadmap for future smart materials. Adv. Sci. *8*, 2100864.

Mannsfeld, S.C., Tee, B.C., Stoltenberg, R.M., Chen, C.V.H., Barman, S., Muir, B.V., Sokolov, A.N., Reese, C., and Bao, Z. (2010). Highly sensitive flexible pressure sensors with microstructured rubber dielectric layers. Nat. Mater. *9*, 859–864.

Manzeli, S., Allain, A., Ghadimi, A., and Kis, A. (2015). Piezoresistivity and strain-induced band gap tuning in atomically thin MoS_2. Nano Lett. *15*, 5330–5335.

Ni, Z.H., Yu, T., Lu, Y.H., Wang, Y.Y., Feng, Y.P., and Shen, Z.X. (2008). Uniaxial strain on graphene: Raman spectroscopy study and band-gap opening. ACS Nano *2*, 2301–2305.

Nie, B., Xing, S., Brandt, J.D., and Pan, T. (2012). Droplet-based interfacial capacitive sensing. Lab Chip *12*, 1110–1118.

Novoselov, K., Mishchenko, A., Carvalho, A., and Neto, A.C. (2016). 2D materials and van der Waals heterostructures. Science *353*, aac9439.

Oviedo, J.P., KC, S., Lu, N., Wang, J., Cho, K., Wallace, R.M., and Kim, M.J. (2014). In situ TEM characterization of shear-stress-induced interlayer sliding in the cross section view of molybdenum disulfide. ACS Nano *9*, 1543–1551.

Pan, K., Ni, Y., He, L., and Huang, R. (2014). Nonlinear analysis of compressed elastic thin films on elastic substrates: from wrinkling to buckle-delamination. Int. J. Sol. Struct. *51*, 3715–3726.

Pang, C., Kim, T.i., Bae, W.G., Kang, D., Kim, S.M., and Suh, K.Y. (2012a). Bioinspired reversible interlocker using regularly arrayed high aspect-ratio polymer fibers. Adv. Mater. *24*, 475–479.

Pang, C., Lee, G.-Y., Kim, T.-i., Kim, S.M., Kim, H.N., Ahn, S.-H., and Suh, K.-Y. (2012b). A flexible and highly sensitive strain-gauge sensor using reversible interlocking of nanofibres. Nat. Mater. *11*, 795.

Pang, Y., Tian, H., Tao, L., Li, Y., Wang, X., Deng, N., Yang, Y., and Ren, T.-L. (2016). Flexible, highly sensitive, and wearable pressure and strain sensors with graphene porous network structure. ACS Appl. Mater. Inter. *8*, 26458–26462.

Pang, Y., Zhang, K., Yang, Z., Jiang, S., Ju, Z., Li, Y., Wang, X., Wang, D., Jian, M., and Zhang, Y. (2018). Epidermis microstructure inspired graphene pressure sensor with random distributed spinosum for high sensitivity and large linearity. ACS Nano *12*, 2346–2354.

Park, J., Kim, M., Lee, Y., Lee, H.S., and Ko, H. (2015). Fingertip skin–inspired microstructured ferroelectric skins discriminate static/dynamic pressure and temperature stimuli. Sci. Adv. *1*, e1500661.

Park, M., Park, Y.J., Chen, X., Park, Y.K., Kim, M.S., and Ahn, J.H. (2016). MoS_2-based tactile sensor for electronic skin applications. Adv. Mater. *28*, 2556–2562.

Qi, J., Lan, Y.-W., Stieg, A.Z., Chen, J.-H., Zhong, Y.-L., Li, L.-J., Chen, C.-D., Zhang, Y., and Wang, K.L. (2015). Piezoelectric effect in chemical vapour deposition-grown atomic-monolayer triangular molybdenum disulfide piezotronics. Nat. Commun. *6*, 1–8.

Qiu, L., Coskun, M.B., Tang, Y., Liu, J.Z., Alan, T., Ding, J., Truong, V.T., and Li, D. (2016). Ultrafast dynamic piezoresistive response of graphene-based cellular elastomers. Adv. Mater. *28*, 194–200.

Rabelo Baccarini, L.M., Rocha e Silva, V.V., de Menezes, B.R., and Caminhas, W.M. (2011). SVM practical industrial application for mechanical faults diagnostic. Expert Syst. Appl. *38*, 6980–6984.

Raju, A.P.A., Lewis, A., Derby, B., Young, R.J., Kinloch, I.A., Zan, R., and Novoselov, K.S. (2014). Wide-area strain sensors based upon graphene-polymer composite coatings probed by Raman spectroscopy. Adv. Funct. Mater. *24*, 2865–2874.

Ren, J., Zhang, W., Wang, Y., Wang, Y., Zhou, J., Dai, L., and Xu, M. (2019). A graphene rheostat for highly durable and stretchable strain sensor. InfoMat *1*, 396–406.

Sanchez, D.A., Dai, Z., Wang, P., Cantu-Chavez, A., Brennan, C.J., Huang, R., and Lu, N. (2018). Mechanics of spontaneously formed nanoblisters trapped by transferred 2D crystals. Proc. Natl. Acad. Sci. U S A *115*, 7884–7889.

Shao, Y., Hayward, V., and Visell, Y. (2016). Spatial patterns of cutaneous vibration during whole-hand haptic interactions. Proc. Natl. Acad. Sci. U S A *113*, 4188–4193.

Shao, W., Ge, Z., and Song, Z. (2020). Bayesian just-in-time learning and its application to industrial soft sensing. IEEE Trans. Ind. Inform. *16*, 2787–2798.

Sharma, S., Chhetry, A., Sharifuzzaman, M., Yoon, H., and Park, J.Y. (2020). Wearable capacitive pressure sensor based on MXene composite nanofibrous scaffolds for reliable human physiological signal acquisition. ACS Appl. Mater. Inter. *12*, 22212–22224.

Shi, J., Wang, L., Dai, Z., Zhao, L., Du, M., Li, H., and Fang, Y. (2018a). Multiscale hierarchical design of a flexible piezoresistive pressure sensor with high sensitivity and wide linearity range. Small *14*, 1800819.

Shi, X., Liu, S., Sun, Y., Liang, J., and Chen, Y. (2018b). Lowering internal friction of 0D–1D–2D ternary nanocomposite-based strain sensor by fullerene to boost the sensing performance. Adv. Funct. Mater. *28*, 1800850.

Shi, X., Wang, H., Xie, X., Xue, Q., Zhang, J., Kang, S., Wang, C., Liang, J., and Chen, Y. (2018c). Bioinspired ultrasensitive and stretchable MXene-based strain sensor via nacre-mimetic microscale "brick-and-mortar" architecture. ACS Nano *13*, 649–659.

Shi, J., Liu, S., Zhang, L., Yang, B., Shu, L., Yang, Y., Ren, M., Wang, Y., Chen, J., and Chen, W. (2020). Smart textile-integrated microelectronic systems for wearable applications. Adv. Mater. *32*, 1901958.

Shih, B., Shah, D., Li, J., Thuruthel, T.G., and Tolley, M.T. (2020). Electronic skins and machine learning for intelligent soft robots. Ence Robotics *5*, eaaz9239.

Shyu, T.C., Damasceno, P.F., Dodd, P.M., Lamoureux, A., Xu, L., Shlian, M., Shtein, M., Glotzer, S.C., and Kotov, N.A. (2015). A kirigami approach to engineering elasticity in nanocomposites through patterned defects. Nat. Mater. *14*, 785.

Song, Z., Ma, T., Tang, R., Cheng, Q., Wang, X., Krishnaraju, D., Panat, R., Chan, C.K., Yu, H., and Jiang, H. (2014). Origami lithium-ion batteries. Nat. Commun. *5*, 3140.

Song, H., Karakurt, I., Wei, M., Liu, N., Chu, Y., Zhong, J., and Lin, L. (2018). Lead iodide nanosheets for piezoelectric energy conversion and strain sensing. Nano Energy *49*, 7–13.

Su, M., Li, F., Chen, S., Huang, Z., Qin, M., Li, W., Zhang, X., and Song, Y. (2015). Nanoparticle based curve arrays for multirecognition flexible electronics. Adv. Mater. *28*, 1369–1374.

Sun, B., McCay, R.N., Goswami, S., Xu, Y., Zhang, C., Ling, Y., Lin, J., and Yan, Z. (2018). Gas-permeable, multifunctional on-skin electronics based on laser-induced porous graphene and sugar-templated elastomer sponges. Adv. Mater. *30*, 1804327.

Sun, Q.J., Zhao, X.H., Zhou, Y., Yeung, C.C., Wu, W., Venkatesh, S., Xu, Z.X., Wylie, J.J., Li, W.J., and Roy, V.A. (2019). Fingertip-skin-inspired highly sensitive and multifunctional sensor with hierarchically structured conductive graphite/polydimethylsiloxane foams. Adv. Funct. Mater. *29*, 1808829.

Tang, R., and Fu, H. (2020). Mechanics of buckled kirigami membranes for stretchable interconnects in island-bridge structures. J. Appl. Mech. *87*, 051002.

Tang, D.-M., Kvashnin, D.G., Najmaei, S., Bando, Y., Kimoto, K., Koskinen, P., Ajayan, P.M., Yakobson, B.I., Sorokin, P.B., and Lou, J. (2014). Nanomechanical cleavage of molybdenum disulphide atomic layers. Nat. Commun. *5*, 3631.

Tao, L.Q., Tian, H., Liu, Y., Ju, Z.Y., Pang, Y., Chen, Y.Q., Wang, D.Y., Tian, X.G., Yan, J.C., and Deng, N.Q. (2017). An intelligent artificial throat with sound-sensing ability based on laser induced graphene. Nat. Commun. *8*, 14579.

Tao, J., Bao, R., Wang, X., Peng, Y., Li, J., Fu, S., Pan, C., and Wang, Z.L. (2019). Self-powered tactile sensor array systems based on the triboelectric effect. Adv. Funct. Mater. *29*, 1806379.

Taylor, D.L., and Panhuis, M.I.H. (2016). Self-healing hydrogels. Adv. Mater. *28*, 9060–9093.

Tee, B.C.-K., Chortos, A., Berndt, A., Nguyen, A.K., Tom, A., McGuire, A., Lin, Z.C., Tien, K., Bae, W.-G., and Wang, H. (2015). A skin-inspired organic digital mechanoreceptor. Science *350*, 313–316.

Terrones, H., Lv, R., Terrones, M., and Dresselhaus, M.S. (2012). The role of defects and doping in 2D graphene sheets and 1D nanoribbons. Rep. Prog. Phys. *75*, 062501.

Tesch da Silva, F.S., da Costa, C.A., Paredes Crovato, C.D., and Righi, R.d.R. (2020). Looking at energy through the lens of Industry 4.0: a systematic literature review of concerns and challenges. Comput. Ind. Eng. *143*, 106426.

Tian, H., Shu, Y., Cui, Y.-L., Mi, W.-T., Yang, Y., Xie, D., and Ren, T.-L. (2014). Scalable fabrication of high-performance and flexible graphene strain sensors. Nanoscale *6*, 699–705.

Truong-Son Dinh, L., An, J., Huang, Y., Quoc, V., Boonruangkan, J., Tuan, T., Kim, S.-W., Sun, G., and Kim, Y.-J. (2019). Ultrasensitive anti-interference voice recognition by bio-inspired skin-attachable self-cleaning acoustic sensors. ACS Nano *13*, 13293–13303.

Tsai, M.-Y., Tarasov, A., Hesabi, Z.R., Taghinejad, H., Campbell, P.M., Joiner, C.A., Adibi, A., and Vogel, E.M. (2015). Flexible MoS_2 field-effect transistors for gate-tunable piezoresistive strain sensors. ACS Appl. Mater. Inter. *7*, 12850–12855.

Tsen, A.W., Brown, L., Levendorf, M.P., Ghahari, F., Huang, P.Y., Havener, R.W., Ruiz-Vargas, C.S., Muller, D.A., Kim, P., and Park, J. (2012). Tailoring electrical transport across grain boundaries in polycrystalline graphene. Science *336*, 1143–1146.

Tseng, P., Napier, B., Zhao, S., Mitropoulos, A.N., Applegate, M.B., Marelli, B., Kaplan, D.L., and Omenetto, F.G. (2017). Directed assembly of bio-inspired hierarchical materials with controlled nanofibrillar architectures. Nat. Nanotechnol. *12*, 474.

Uzun, S., Seyedin, S., Stoltzfus, A.L., Levitt, A.S., Alhabeb, M., Anayee, M., Strobel, C.J., Razal, J.M., Dion, G., and Gogotsi, Y. (2019). Knittable and washable multifunctional mXene-coated cellulose yarns. Adv. Funct. Mater. *29*, 1905015.

Wagner, S., Yim, C., McEvoy, N., Kataria, S., Yokaribas, V., Kuc, A., Pindl, S., Fritzen, C.-P., Heine, T., and Duesberg, G.S. (2018). Highly sensitive electromechanical piezoresistive pressure sensors based on large-area layered $PtSe_2$ films. Nano Lett. *18*, 3738–3745.

Wan, S., Bi, H., Zhou, Y., Xie, X., Su, S., Yin, K., and Sun, L. (2017). Graphene oxide as high-performance dielectric materials for capacitive pressure sensors. Carbon *114*, 209–216.

Wang, Y., Yang, R., Shi, Z., Zhang, L., Shi, D., Wang, E., and Zhang, G. (2011). Super-elastic graphene ripples for flexible strain sensors. ACS Nano *5*, 3645–3650.

Wang, Y., Wang, L., Yang, T., Li, X., Zang, X., Zhu, M., Wang, K., Wu, D., and Zhu, H. (2014). Wearable and highly sensitive graphene strain sensors for human motion monitoring. Adv. Funct. Mater. *24*, 4666–4670.

Wang, W., Dai, S., Li, X., Yang, J., Srolovitz, D.J., and Zheng, Q. (2015a). Measurement of the cleavage energy of graphite. Nat. Commun. *6*, 7853.

Wang, W., Yang, T., Zhu, H., and Zheng, Q. (2015b). Bio-inspired mechanics of highly sensitive stretchable graphene strain sensors. Appl. Phys. Lett. *106*, 171903.

Wang, Y., Yang, T., Lao, J., Zhang, R., Zhang, Y., Zhu, M., Li, X., Zang, X., Wang, K., and Yu, W. (2015c). Ultra-sensitive graphene strain sensor for sound signal acquisition and recognition. Nano Res. *8*, 1627–1636.

Wang, X., He, X., Zhu, H., Sun, L., Fu, W., Wang, X., Hoong, L.C., Wang, H., Zeng, Q., and Zhao, W. (2016). Subatomic deformation driven by vertical piezoelectricity from CdS ultrathin films. Sci. Adv. *2*, e1600209.

Wang, G., Dai, Z., Wang, Y., Tan, P., Liu, L., Xu, Z., Wei, Y., Huang, R., and Zhang, Z. (2017a). Measuring interlayer shear stress in bilayer graphene. Phys. Rev. Lett. *119*, 036101.

Wang, G., Li, X., Wang, Y., Zheng, Z., Dai, Z., Qi, X., Liu, L., Cheng, Z., Xu, Z., and Tan, P. (2017b). Interlayer coupling behaviors of boron doped multilayer graphene. J. Phys. Chem. C *121*, 26034–26043.

Wang, Y., Wang, Y., and Yang, Y. (2018). Graphene–polymer nanocomposite-based redox-induced electricity for flexible self-powered strain sensors. Adv. Energy Mater. *8*, 1800961.

Wang, G., Dai, Z., Xiao, J., Feng, S., Weng, C., Liu, L., Xu, Z., Huang, R., and Zhang, Z. (2019a). Bending of multilayer van der waals materials. Phys. Rev. Lett. *123*, 116101.

Wang, K., Lou, Z., Wang, L., Zhao, L., Zhao, S., Wang, D., Han, W., Jiang, K., and Shen, G. (2019b). Bioinspired interlocked structure-induced high deformability for two-dimensional titanium carbide (MXene)/natural microcapsule-based flexible pressure sensors. ACS Nano *13*, 9139–9147.

Wang, H., Wang, H., Wang, Y., Su, X., Wang, C., Zhang, M., Jian, M., Xia, K., Liang, X., and Lu, H. (2020a). Laser writing of Janus graphene/kevlar textile for intelligent protective clothing. ACS Nano *14*, 3219–3226.

Wang, M., Yan, Z., Wang, T., Cai, P., Gao, S., Zeng, Y., Wan, C., Wang, H., Pan, L., Yu, J., et al. (2020b). Gesture recognition using a bioinspired learning architecture that integrates visual data with somatosensory data from stretchable sensors. Nat. Electron. *3*, 563–570.

Wang, M., Wang, T., Luo, Y., He, K., Pan, L., Li, Z., Cui, Z., Liu, Z., Tu, J., and Chen, X. (2021). Fusing stretchable sensing technology with machine learning for human-machine interfaces. Adv.Funct.Mater. *31*, 2008807.

Webb, R.C., Bonifas, A.P., Behnaz, A., Zhang, Y., Yu, K.J., Cheng, H., Shi, M., Bian, Z., Liu, Z., and Kim, Y.-S. (2013). Ultrathin conformal devices for precise and continuous thermal characterization of human skin. Nat. Mater. *12*, 938.

Webb, R.C., Ma, Y., Krishnan, S., Li, Y., Yoon, S., Guo, X., Feng, X., Shi, Y., Seidel, M., and Cho, N.H. (2015). Epidermal devices for noninvasive, precise, and continuous mapping of macrovascular and microvascular blood flow. Sci. Adv. *1*, e1500701.

Wei, Y., Wang, B., Wu, J., Yang, R., and Dunn, M.L. (2013). Bending rigidity and Gaussian bending stiffness of single-layered graphene. Nano Lett. *13*, 26–30.

Wei, X., Meng, Z., Ruiz, L., Xia, W., Lee, C., Kysar, J.W., Hone, J.C., Keten, S., and Espinosa, H.D. (2016). Recoverable slippage mechanism in multilayer graphene leads to repeatable energy dissipation. ACS Nano *10*, 1820–1828.

Won, Y., Kim, A., Yang, W., Jeong, S., and Moon, J. (2014). A highly stretchable, helical copper nanowire conductor exhibiting a stretchability of 700. NPG Asia Mater. *6*, e132.

Wu, W., Wang, L., Li, Y., Zhang, F., Lin, L., Niu, S., Chenet, D., Zhang, X., Hao, Y., and Heinz, T.F. (2014). Piezoelectricity of single-atomic-layer MoS_2 for energy conversion and piezotronics. Nature *514*, 470–474.

Xiang, C., Liu, C., Hao, C., Wang, Z., Che, L., and Zhou, X. (2017). A self-powered acceleration sensor with flexible materials based on triboelectric effect. Nano Energy *31*, 469–477.

Xiao, L., Zhu, C., Xiong, W., Huang, Y., and Yin, Z. (2018). The conformal design of an island-bridge structure on a non-developable surface for stretchable electronics. Micromachines *9*, 392.

Xiong, W., Zhu, C., Guo, D., Hou, C., Yang, Z., Xu, Z., Qiu, L., Yang, H., Li, K., and Huang, Y. (2021). Bio-inspired, intelligent flexible sensing skin for multifunctional flying perception. Nano Energy *90*, 106550.

Xu, Y., Guo, Z., Chen, H., Yuan, Y., Lou, J., Lin, X., Gao, H., Chen, H., and Yu, B. (2011). In-plane and tunneling pressure sensors based on graphene/hexagonal boron nitride heterostructures. Appl. Phys. Lett. *99*, 133109.

Xu, S., Zhang, Y., Cho, J., Lee, J., Huang, X., Jia, L., Fan, J.A., Su, Y., Su, J., and Zhang, H. (2013). Stretchable batteries with self-similar serpentine interconnects and integrated wireless recharging systems. Nat. Commun. *4*, 1–8.

Xu, C., Xue, T., Guo, J., Qin, Q., Wu, S., Song, H., and Xie, H. (2015). An experimental investigation on the mechanical properties of the interface between large-sized graphene and a flexible substrate. J. Appl. Phys. *117*, 164301.

Xu, C., Xue, T., Qiu, W., and Kang, Y. (2016). Size effect of the interfacial mechanical behavior of graphene on a stretchable substrate. ACS Appl. Mater. Inter. *8*, 27099–27106.

Xu, W., Yang, T., Qin, F., Gong, D., Du, Y., and Dai, G. (2019). A sprayed graphene pattern-based flexible strain sensor with high sensitivity and fast response. Sensors *19*, 1077.

Yan, Z., Han, M., Yang, Y., Nan, K., Luan, H., Luo, Y., Zhang, Y., Huang, Y., and Rogers, J.A. (2017). Deterministic assembly of 3D mesostructures in advanced materials via compressive buckling: a short review of recent progress. Extreme Mech. Lett. *11*, 96–104.

Yang, C., and Suo, Z. (2018). Hydrogel ionotronics. Nat. Rev. Mater. *3*, 125–142.

Yang, T., Wang, W., Zhang, H., Li, X., Shi, J., He, Y., Zheng, Q.-s., Li, Z., and Zhu, H. (2015). Tactile sensing system based on arrays of graphene woven microfabrics: electromechanical behavior and electronic skin application. ACS Nano *9*, 10867–10875.

Yang, T., Jiang, X., Zhong, Y., Zhao, X., Lin, S., Li, J., Li, X., Xu, J., Li, Z., and Zhu, H. (2017a). A wearable and highly sensitive graphene strain sensor for precise home-based pulse wave monitoring. ACS Sensors *2*, 967–974.

Yang, T., Zhong, Y., Tao, D., Li, X., Zang, X., Lin, S., Jiang, X., Li, Z., and Zhu, H. (2017b). Integration of graphene sensor with electrochromic device on modulus-gradient polymer for instantaneous strain visualization. 2D Mater. *4*, 035020.

Yang, Z., Pang, Y., Han, X.-l., Yang, Y., Ling, J., Jian, M., Zhang, Y., Yang, Y., and Ren, T.-L. (2018). Graphene textile strain sensor with negative resistance variation for human motion detection. ACS Nano *12*, 9134–9141.

Yang, J., Luo, S., Zhou, X., Li, J., Fu, J., Yang, W., and Wei, D. (2019a). Flexible, tunable, and ultrasensitive capacitive pressure sensor with microconformal graphene electrodes. ACS Appl. Mater. Inter. *11*, 14997–15006.

Yang, Y., Song, Y., Bo, X., Min, J., and Gao, W. (2019b). A laser-engraved wearable sensor for sensitive detection of uric acid and tyrosine in sweat. Nat. Biotechnol. *38*, 1–8.

Yang, T., Wang, W., Huang, Y., Jiang, X., and Zhao, X. (2020). Accurate monitoring of small strain for timbre recognition via ductile fragmentation of functionalized graphene multilayers. ACS Appl. Mater. Inter. *12*, 57352–57361.

Yang, Z., Li, H., Zhang, S., Lai, X., and Zeng, X. (2021). Superhydrophobic MXene@ carboxylated carbon nanotubes/carboxymethyl chitosan aerogel for piezoresistive pressure sensor. Chem. Eng. J. *425*, 130462.

Yao, H., Li, P., Cheng, W., Yang, W., Yang, Z., Ali, H.P.A., Guo, H., and Tee, B.C. (2020). Environment-resilient graphene vibrotactile sensitive sensors for machine intelligence. ACS Mater. Lett. *2*, 986–992.

Yu, Q., Jauregui, L.A., Wu, W., Colby, R., Tian, J., Su, Z., Cao, H., Liu, Z., Pandey, D., and Wei, D. (2011). Control and characterization of individual grains and grain boundaries in graphene grown by chemical vapour deposition. Nat. Mater. *10*, 443.

Zha, J.-W., Zhang, B., Li, R.K., and Dang, Z.-M. (2016). High-performance strain sensors based on functionalized graphene nanoplates for damage monitoring. Compos. Sci. Technol. *123*, 32–38.

Zhang, Y., and Tao, T.H. (2019). Skin-friendly electronics for acquiring human physiological signatures. Adv. Mater. *31*, 1905767.

Zhang, Z., Zou, X., Crespi, V.H., and Yakobson, B.I. (2013). Intrinsic magnetism of grain boundaries in two-dimensional metal dichalcogenides. ACS Nano *7*, 10475–10481.

Zhang, Q., Jiang, T., Ho, D., Qin, S., Yang, X., Cho, J.H., Sun, Q., and Wang, Z.L. (2018a). Transparent and self-powered multistage sensation matrix for mechanosensation application. ACS Nano *12*, 254–262.

Zhang, H., Chhowalla, M., and Liu, Z. (2018b). 2D nanomaterials: graphene and transition metal dichalcogenides. Chem. Soc. Rev. *47*, 3015–3017.

Zhang, Y., Chen, Y., Man, T., Huang, D., and Li, Z. (2019). High resolution non-invasive intraocular pressure monitoring by use of graphene woven fabrics on contact lens. Microsyst.Nanoeng. *5*, 1–8.

Zhang, M., Guo, R., Chen, K., Wang, Y., Niu, J., Guo, Y., Zhang, Y., Yin, Z., Xia, K., and Zhou, B. (2020). Microribbons composed of directionally self-assembled nanoflakes as highly stretchable ionic neural electrodes. Proc. Nat. Acad. Sci. U S A *117*, 14667–14675.

Zhang, L., Zhang, S., Wang, C., Zhou, Q., Zhang, H., and Pan, G.-B. (2021). Highly sensitive capacitive flexible pressure sensor based on a high-permittivity MXene nanocomposite and 3D network electrode for wearable electronics. ACS Sensors *6*, 2630–2641.

Zhao, J., He, C., Yang, R., Shi, Z., Cheng, M., Yang, W., Xie, G., Wang, D., Shi, D., and Zhang, G. (2012). Ultra-sensitive strain sensors based on piezoresistive nanographene films. Appl. Phys. Lett. *101*, 063112.

Zhao, J., Wang, G., Yang, R., Lu, X., Cheng, M., He, C., Xie, G., Meng, J., Shi, D., and Zhang, G. (2015). Tunable piezoresistivity of nanographene films for strain sensing. ACS Nano *9*, 1622–1629.

Zhao, X., Chen, B., Wei, G., Wu, J.M., Han, W., and Yang, Y. (2019). Polyimide/graphene nanocomposite foam-based wind-driven triboelectric nanogenerator for self-powered pressure sensor. Adv. Mater. Technol. *4*, 1800723.

Zheng, L., Wang, X., Jiang, H., Xu, M., Huang, W., and Liu, Z. (2021a). Recent progress of flexible electronics by 2D transition metal dichalcogenides. Nano Res. https://doi.org/10.1007/s12274-021-3779-z.

Zheng, Y., Yin, R., Zhao, Y., Liu, H., Zhang, D., Shi, X., Zhang, B., Liu, C., and Shen, C. (2021b). Conductive MXene/cotton fabric based pressure sensor with both high sensitivity and wide sensing range for human motion detection and E-skin. Chem. Eng. J. *420*, 127720.

Zhou, W., Zou, X., Najmaei, S., Liu, Z., Shi, Y., Kong, J., Lou, J., Ajayan, P.M., Yakobson, B.I., and Idrobo, J.-C. (2013). Intrinsic structural defects in monolayer molybdenum disulfide. Nano Lett. *13*, 2615–2622.

Zhou, Z.H., Chen, K., Li, X.S., Zhang, S.L., Wu, Y.F., Zhou, Y.H., Meng, K.Y., Sun, C.C., He, Q., Fan, W.J., et al. (2020). Sign-to-speech translation using machine-learning-assisted stretchable sensor arrays. Nat. Electron. *3*, 571–578.

Zhu, Y., and Xu, F. (2012). Buckling of aligned carbon nanotubes as stretchable conductors: a new manufacturing strategy. Adv. Mater. *24*, 1073–1077.

Zhu, W., Low, T., Perebeinos, V., Bol, A.A., Zhu, Y., Yan, H., Tersoff, J., and Avouris, P. (2012). Structure and electronic transport in graphene wrinkles. Nano Lett. *12*, 3431–3436.

Zhu, B., Niu, Z., Wang, H., Leow, W.R., Wang, H., Li, Y., Zheng, L., Wei, J., Huo, F., and Chen, X. (2014). Microstructured graphene arrays for highly sensitive flexible tactile sensors. Small *10*, 3625–3631.

Zhu, H., Wang, Y., Xiao, J., Liu, M., Xiong, S., Wong, Z.J., Ye, Z., Ye, Y., Yin, X., and Zhang, X. (2015). Observation of piezoelectricity in free-standing monolayer MoS_2. Nat. Nanotechnol. *10*, 151–155.

Zhu, P., Du, H., Hou, X., Lu, P., Wang, L., Huang, J., Bai, N., Wu, Z., Fang, N.X., and Guo, C.F. (2021). Skin-electrode iontronic interface for mechanosensing. Nat. Commun. *12*, 1–10.